Original Article

Impaired nitric oxide production and increased blood pressure in systemic heterozygous ATP2B1 null mice

Akira Fujiwara[a], Nobuhito Hirawa[b], Megumi Fujita[a], Yusuke Kobayashi[a], Yuki Okuyama[a], Keisuke Yatsu[a], Mari Katsumata[b], Yuichiro Yamamoto[b], Naoaki Ichihara[a], Sanae Saka[b], Yoshiyuki Toya[a], Gen Yasuda[b], Yoshio Goshima[c], Yasuharu Tabara[d], Tetsuro Miki[e], Hirotsugu Ueshima[f], Yoshihiro Ishikawa[g], and Satoshi Umemura[a]

Background: In the 'Millennium Genome Project', we identified ATP2B1 as a gene responsible for hypertension through single-nucleotide polymorphism analysis. The ATP2B1 gene encodes the plasma membrane calcium ATPase isoform 1, which contributes to the maintenance of intracellular calcium homeostasis by removing calcium ions.

Method: Since ATP2B1 knockout mice are reported to be embryo-lethal, we generated systemic heterozygous ATP2B1 null ($ATP2B1^{+/-}$) mice, and evaluated the implication of ATP2B1 in blood pressure.

Results: $ATP2B1^{+/-}$ mice revealed significantly higher SBP as measured by a radiotelemetric method. Phenylephrine-induced vasoconstriction was significantly increased in vascular rings from $ATP2B1^{+/-}$ mice, and the difference in this contraction disappeared in the presence of a nitric oxide synthase (NOS) inhibitor. Vasorelaxation to acetylcholine was significantly attenuated in vascular rings from $ATP2B1^{+/-}$ mice. In addition, cultured endothelial cells of $ATP2B1^{+/-}$ mice showed that the phosphorylation (Ser-1177) level of endothelial NOS protein was significantly lower, and nitric oxide production in endothelial cells and aorta was lower compared with those in control mice. In contrast, neural NOS expression in vascular smooth muscle cells from $ATP2B1^{+/-}$ mice and control mice were not significantly different.

Conclusion: These results suggest that decreased ATP2B1 gene expression is associated with impaired endothelial NOS activity and nitric oxide production, and the ATP2B1 gene plays a crucial role in the regulation of blood pressure.

Keywords: ATP2B1, cre-loxP system, endothelial nitric oxide synthase, hypertension, nitric oxide

Abbreviations: $ATP2B1^{+/-}$ mice, systemic heterozygous ATP2B1 null mice; eNOS, endothelial nitric oxide synthase; L-NAME, *N*ω-nitro-L-arginine methyl ester; NOx, nitrate/nitrite; NCX, sodium/calcium exchanger; nNOS, neural nitric oxide synthase; NOS, nitric oxide synthase; PMCA, plasma membrane calcium ATPase isoform; qRT-PCR, quantitative reverse transcription-PCR; SERCA, sarco-endoplasmic reticulum Ca^{2+}-ATPase; SNP, single-nucleotide polymorphism; VSMC, vascular smooth muscle cell

INTRODUCTION

Hypertension is a major cardiovascular risk factor affecting more than 25% of the adult population according to a recent worldwide analysis, and is the leading contributor to global mortality [1]. As with other multifactorial disorders, hypertension is a complex genetic disorder caused by interaction between several risk genes and environmental factors [2,3]. To date, large-scale genome-wide association studies have attempted to identify genetic markers for hypertension. However, although many studies have been conducted all over the world, they have produced inconsistent results. In the 'Millennium Genome Project', we identified ATP2B1 as a gene responsible for hypertension in Japanese through single-nucleotide polymorphism (SNP) analysis [4]. These SNPs have been replicated in individuals of European descent [5], Korean descent [6], other Japanese descents [7], and the whole world [8]. The ATP2B1 gene encodes the plasma membrane calcium ATPase 1 (PMCA1), which contributes to the maintenance of appropriate cytoplasmic calcium levels by removing calcium ions from the cell to the extracellular environment [9]. In particular, PMCA, sarco-endoplasmic reticulum Ca^{2+}-ATPase (SERCA) and sodium/calcium exchanger (NCX) play a crucial role in intracellular calcium homeostasis. PMCA comprises four different isoforms (PMCA1–4) that are encoded by four independent genes. PMCA1 and PMCA4 are expressed ubiquitously, whereas PMCA2 and PMCA3 are mainly

Journal of Hypertension 2014, 32:1415–1423

[a]Department of Medical Science and Cardiorenal Medicine, Yokohama City University Graduate School of Medicine, [b]Department of Nephrology and Hypertension, Yokohama City University Medical Center, [c]Molecular Pharmacology and Neurobiology, Yokohama City University Graduate School of Medicine, Yokohama, [d]Center for Genomic Medicine, Kyoto University Graduate School of Medicine, Kyoto, [e]Department of Geriatric Medicine, Ehime University Graduate School of Medicine, Toon, [f]Department of Health Science, Shiga University of Medical Science, Otsu and [g]Cardiovascular Research Institute, Yokohama City University Graduate School of Medicine, Yokohama, Japan

Correspondence to Nobuhito Hirawa, MD, PhD, Department of Nephrology and Hypertension, Yokohama City University Medical Center, 45-7, Urafune-cho, Minami-ku, Yokohama 232-0024, Japan. Tel: +81 45 261 5656; fax: +81 45 253 9955; e-mail: hirawa@yokohama-cu.ac.jp

Received 18 August 2013 **Revised** 17 March 2014 **Accepted** 17 March 2014

J Hypertens 32:1415–1423

DOI:10.1097/HJH.0000000000000206

present in neuronal tissue [10,11]. Since the ATP2B1 null mutant mouse is embryo-lethal [12], we attempted to make a conditional knockout mouse model of ATP2B1 using the Cre-loxP system. We reported previously that mice with ATP2B1 knockout in vascular smooth muscle cells (VSMCs) showed increased blood pressure [13,14]. However, this could not address the role of ATP2B1 in the whole body. So we generated systemic heterozygous ATP2B1 null ($ATP2B1^{+/-}$) mice, and evaluated the implication of ATP2B1 in blood pressure. Moreover, there have been several reports on the relationship between PMCAs and nitric oxide synthase (NOS) in recent years. Previous studies have shown that PMCAs inhibit endothelial NOS (eNOS) activity [15], and PMCA4 regulates neural NOS (nNOS) [16,17]. In this study, we also examined whether reduced ATP2B1 gene expression affects NOS activity and nitric oxide production.

METHODS

Animal care

Animals were housed under a 12-h light-dark cycle at a temperature of 25°C. Mice were studied at 3 months of age and fed a normal-salt diet with free access to drinking water. Experiments were conducted under the guidelines for animal experiments set by the Animal Experiment Committee of Yokohama City University School of Medicine.

Creation of systemic heterozygous ATP2B1 null ($ATP2B1^{+/-}$) mice

$ATP2B1^{loxP/loxP}$ mice were generated using the Cre-loxP and flippase recombination enzyme-flippase recognition target recombination system. ATP2B1 is encoded by 21 exons on chromosome 10, and mice systemically lacking exon 10 were reported to be embryo-lethal [12]. We, therefore, designed a vector to knock out exon 10 of the ATP2B1 gene. The detailed technical strategy for conditional knockout mouse generation is described previously [13].

Tie2 promotor can cause noncell-specific deletion of floxed alleles through the germ line activation. Normally, two successive rounds of breeding are performed to generate mice carrying two floxed target-gene alleles and a transgene expressing Cre-recombinase tissue-specifically. However, this causes the conversion of the floxed allele to a null allele in the germ line, which is transmitted to offspring, which can result in global deletion irrespective of their Cre-recombinase genotype. Therefore, germ-line activation of the Tie2 promotors can cause noncell-specific deletion of floxed alleles with a fixed probability [18]. $ATP2B1^{+/loxP}$:Tie2-Cre mice were created by mating $ATP2B1^{loxP/loxP}$ female mice with transgenic mice expressing Cre recombinase under control of the murine Tie2 promotor (Tie2-Cre mice) [19] [B6.Cg-Tg(Tie2-Cre)1Ywa/J, stock No.008863, Jackson Laboratory]. $ATP2B1^{+/loxP}$:Tie2-Cre male offspring were then crossed with $ATP2B1^{loxP/loxP}$ female mice, and we created systemic heterozygous ATP2B1 null [$ATP2B1^{+/-}$:Tie2-Cre(-)] mice and genetic control [$ATP2B1^{+/+}$:Tie2-Cre(-)] mice.

Cell culture

The aorta was dissected out from the aortic arch to the abdominal aorta and immersed in 10% fetal bovine serum (FBS)-Dulbecco's Modified Eagle Medium (DMEM) containing 1000 U/ml heparin (Sigma-Aldrich). A 24-gauge cannula was inserted into the proximal portion of the aorta. The other side was tied, and the lumen was filled with a solution of collagenase type II (2 mg/ml, dissolved in serum-free DMEM). After incubation at 37°C for 45 min, endothelial cells were removed from the aorta by flushing with 5 ml DMEM containing 10% FBS and cultured in a 35-mm collagen type I-coated dish. On the contrary, the aorta is cut into pieces and put inside onto a 60 mm gelatin dish. VSMCs were cultured for approximately 10 days [20].

Real-time quantitative reverse transcription-PCR analysis

Total RNA was extracted from the brain, heart, lung, aorta, kidney, liver, spleen, skeletal muscle, cultured VSMCs, and cultured endothelial cells with ISOGEN (Nippon Gene). cDNA was synthesized using the SuperScript III First Strand System (Invitrogen). Real-time quantitative reverse transcription-PCR (qRT-PCR) was performed by incubating the reverse transcription product with TaqMan PCR Master Mix (Applied Biosystems) and a designed TaqMan probe (ATP2B1: Mm01245796_m1, ATP2B4: Mm01285597_m1, NCX1: Mm01232254_m1; Applied Biosystems) [21]. RNA quantities were expressed relative to the 18S (4319413E; Applied Biosystems) mRNA control.

Western blot analysis

Western blot analysis was performed as described previously [13]. Briefly, tissue extracts were used for electrophoresis, and membranes (Millipore) were incubated with anti-PMCA1 antibody (recognizes exon10; Unitech), anti-eNOS antibody (Abcam), anti-phospho eNOS antibody (Ser-1177; Cell Signaling Technology), anti-nNOS antibody (Thermo Scientific), anti-β-actin antibody (Abcam) or anti-Flotillin-2 antibody (Cell Signaling Technology) and subjected to enhanced chemiluminescence (Amersham Biosciences). The images were analyzed quantitatively using a FUJI LAS3000 Image Analyzer (FUJI Film) to determine each protein level. Kidney and liver tissues were fractionated into membrane and cytoplasmic components.

Blood pressure measurements by radiotelemetric method

Direct blood pressure measurement was performed by a radiotelemetric method in which a blood pressure transducer (PA-C10, Data Sciences International) was inserted into the left carotid artery at 3 months of age. The mice were anesthetized with 2% isoflurane. Ten days after transplantation, each mouse was placed in a metabolic cage (TECNIPLAST) and acclimatized for 3 days on a normal-salt diet (0.3% NaCl). Then direct blood pressure, heart rate and locomotor activity were recorded every 5 min by the Dataquest ART Gold Acquisition software (Data Sciences International) under a 12-h light-dark cycle, as described previously [22].

Measurement of intracellular calcium concentration in cultured vascular smooth muscle cells

Briefly, $ATP2B1^{+/-}$ or control VSMCs grown on 25-mm cover slips were loaded with the calcium-specific dye

Fura-2-acetoxymethyl ester (2.5 μmol/l; Invitrogen) and 0.01% Pluronic acid (Invitrogen) for 30 min at 37°C. After washing with the Hank balanced salt solution, cells were incubated for 20 min at 37°C in the Hank balanced salt solution (Invitrogen) to allow complete hydrolysis of Fura-2-acetoxymethyl ester to Fura-2. Emissions fluorescence was measured with a CCD camera (U-PMTV1X, Olympus) at a wavelength of 510 nm. Real-time shifts in Fura-2 ratio fluorescence (ratio of emissions: F340:F380), indicating changes in intracellular calcium concentration, were recorded before, during, and after stimulating VSMCs with 1 μmol/l phenylephrine, and we used calcium ionophore A23187 (Calbiochem) as positive control for the accuracy of the intracellular calcium concentrations. Summary data represent the average difference in basal condition and the peak increase in phenylephrine-induced intracellular calcium concentration.

Isometric tension of vascular rings

We measured isometric tension of abdominal aortic vascular rings from ATP2B1$^{+/-}$ mice and control mice, as described previously [13,23]. Phenylephrine (Sigma-Aldrich) and potassium-enriched solution were added to stimulate vasoconstriction. Acetylcholine (Sigma-Aldrich) and sodium nitroprusside (Sigma-Aldrich) were added to stimulate vasorelaxation during constriction to the phenylephrine (0.1–1 μmol/l), which evoke a sub-maximal constriction. To eliminate the effect of NOS, the vascular rings were treated with 1 mmol/l *N*ω-nitro-L-arginine methyl ester (L-NAME; NOS inhibitor, Sigma-Aldrich) 5 min before phenylephrine was applied. At the end of all experiments, vasoconstriction of vascular rings was induced by potassium-enriched solutions containing (in mmol/l): KCl 120, $CaCl_2$ 2.5, $MgSO_4$ 1.17, $NaHCO_3$ 25, KH_2PO_4 1.18, EDTA 0.027, glucose 5.5.

Evaluation of nitric oxide production by measuring nitrate/nitrite

After reaching sub-confluence, endothelial cells in 6-well dishes were washed gently three times with phosphate-buffered saline and incubated in 1 ml DMEM without phenol red for 24 h. The aorta rings were cut into 10-mm segments and incubated in 0.5 ml DMEM without phenol red for 24 h. The supernatants were used for nitrate/nitrite (NOx) measurement. Concentrations of NOx in culture media were determined by the Griess method (Griess Reagent Kit, Dojindo) [24].

Statistical analysis

For statistical analysis of differences among groups, unpaired Student's *t* test or analysis of variance (ANOVA) followed by Scheffe *F* test was used. All of the quantitative data are expressed as mean ± SEM. Values of *P* less than 0.05 were considered statistically significant.

RESULTS

Generation of ATP2B1$^{+/-}$ mice

ATP2B1$^{+/-}$ mice were generated by mating ATP2B1$^{+/+}$: Tie2-Cre male mice with ATP2B1$^{loxP/loxP}$ female mice. These mice were born and grew normally into adulthood with no detectable abnormalities. qRT-PCR analysis showed approximately 70% lower ATP2B1 mRNA levels in tissues (brain, heart, lung, aorta, kidney, liver, spleen and skeletal muscle) from ATP2B1$^{+/-}$ mice compared with control mice (Fig. 1a). The levels of ATP2B1 mRNA isolated from VSMCs and endothelial cells of ATP2B1$^{+/-}$ mice were also reduced by approximately 70% compared with control mice (Fig. 1b). RT-PCR analysis demonstrated a deletion of exon 10 in ATP2B1$^{+/-}$ VSMCs (Fig. 1c and Supplementary Figure 1, http://links.lww.com/HJH/A354). The western blot analysis showed that expression of PMCA1 protein in VSMCs, kidney and liver from ATP2B1$^{+/-}$ mice was significantly lower than that from control mice (Fig. 1d). Body weight was measured at 6, 8, 10, and 12 weeks after birth. As seen in Fig. 1e, there was no difference in changes in body weight between ATP2B1$^{+/-}$ mice and control mice. Heart weight/body weight ratios were increased in ATP2B1$^{+/-}$ mice compared with that in control mice at 3 months of age (4.98 ± 0.12 versus 4.46 ± 0.12 mg/g body weight; $P < 0.05$; Fig. 1f).

ATP2B1$^{+/-}$ mice showed higher blood pressure

Figure 2 shows the results of SBP and heart rate measurements from conscious, unrestrained ATP2B1$^{+/-}$ mice and genetic control mice at 3 months of age by radiotelemetric method (Supplementary Figure 2, http://links.lww.com/HJH/A354). There was a consistent increase in SBP of ATP2B1$^{+/-}$ mice compared with control mice during the entire day (130 ± 3 versus 121 ± 2 mmHg; $P < 0.05$) and the dark phase (134 ± 3 versus 123 ± 3 mmHg; $P < 0.05$) under a normal-salt diet. On the contrary, there was no significant difference in heart rate between the two groups (576 ± 11 versus 573 ± 12 b.p.m.). DBP, mean blood pressure, pulse pressure and locomotor activity were not significantly different from ATP2B1$^{+/-}$ mice and control mice measured by radiotelemetric method (Supplementary Figure 3, http://links.lww.com/HJH/A354).

Expression of calcium-regulated genes

mRNA expression of ATP2B4 and NCX1 was evaluated in the aorta, VSMCs and endothelial cells. ATP2B1$^{+/-}$ mice did not show significant alteration of ATP2B4 and NCX1 mRNA expression (Fig. 3a,b).

Calcium concentration in ATP2B1$^{+/-}$ vascular smooth muscle cells

To investigate whether intracellular calcium concentration was altered in ATP2B1$^{+/-}$ VSMCs, we performed fura-2/AM fluorescence assay. As shown in Fig. 4, phenylephrine-induced intracellular calcium concentration was higher in ATP2B1$^{+/-}$ VSMCs than that in control VSMCs (F340/F380 ratio of ATP2B1$^{+/-}$ VSMCs at peak increase: 2.41 ± 0.16; F340/F380 ratio of control VSMCs at peak increase: 1.47 ± 0.08; $P < 0.01$).

Vasoconstriction and vasorelaxation in ATP2B1$^{+/-}$ mice

The vasoconstrictor response of vascular rings to phenylephrine was examined. In response to 1, 10, and 100 nmol/l,

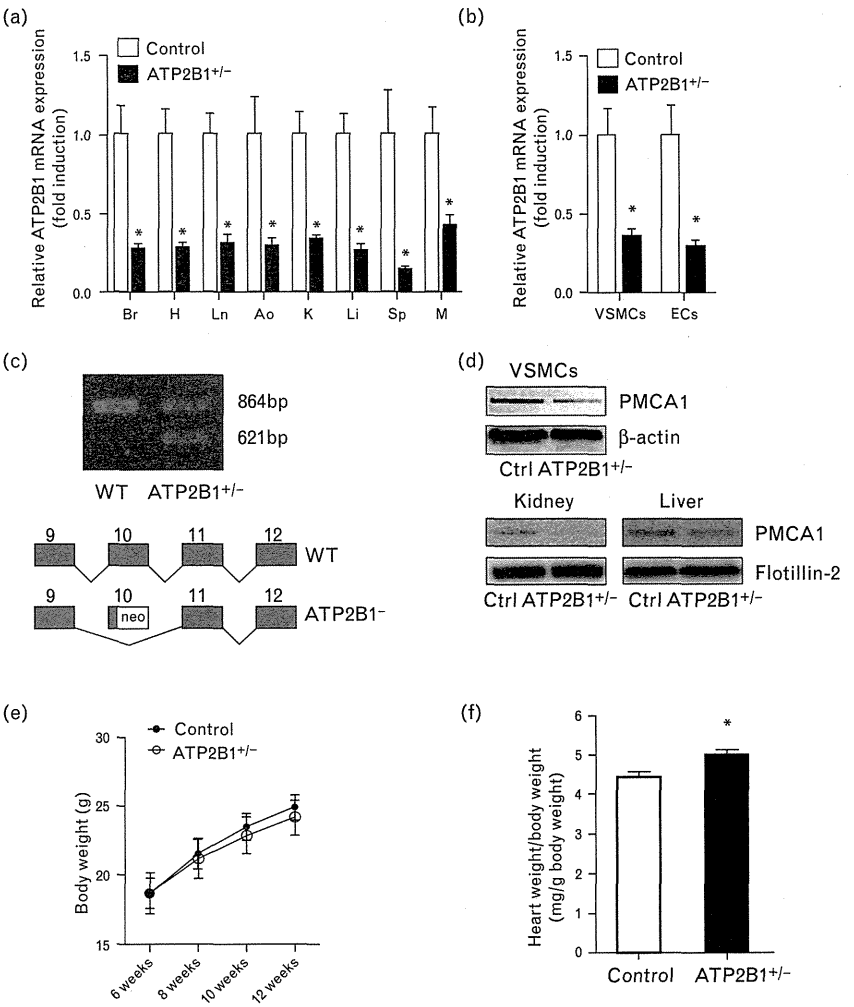

FIGURE 1 ATP2B1 mRNA expression in tissues (a) and isolated cells (b) of 3-month-old mice as quantified by quantitative reverse transcription-PCR (qRT-PCR) using exon 10 and 11 amplification ($n=6$ for each group). (c) RT-PCR analysis of mRNA. First-strand cDNA was prepared from total RNA of ATP2B1$^{+/-}$ or control mice VSMCs using *oligo(dT) primers and reverse transcriptase. The cDNA was amplified by PCR using the forward primer* 5′-AAGACCATGGCTTGCAGAGT-3′ *(located in the exon 9) and* reverse primer 5′-TCAGGCCTCACAGGATCTTC-3′ (located in the exon 12). The presence of wild-type ATP2B1 and recombined ATP2B1 was determined using the forward primer and reverse primer, generating products of 864 kb for wild type and 621 bp for recombined ATP2B1. (d) Representative western blot of PMCA1, β-actin and Flotillin-2 protein expression in VSMCs, kidney and liver from ATP2B1$^{+/-}$ mice and control mice. (e) Growth curve of ATP2B1$^{+/-}$ mice and control mice. All data were collected from male mice ($n=6$ for each group). (f) Heart weight/body weight ratios in ATP2B1$^{+/-}$ mice and control mice at 3 months of age ($n=8$ for each group). *$P<0.05$ versus the control group. Ao, aorta; Br, brain; ECs, endothelial cells; H, heart; K, kidney; L, liver; Ln, lung; M, skeletal muscle; PMCA1, plasma membrane calcium ATPase isoform 1; qRT-PCR, quantitative reverse transcription-PCR; Sp, spleen; VSMCs, vascular smooth muscle cells; WT, wild type.

and 1 μmol/l phenylephrine, vascular rings from ATP2B1$^{+/-}$ mice contracted more strongly than those from control mice (102 ± 7 versus $55\pm11\%$; $P<0.05$; Fig. 5a). Moreover, to clarify whether the phenylephrine-induced contractile response would be affected by nitric oxide production, the effect of L-NAME was examined. In the presence of 1 mmol/l L-NAME, the contractile ability increased in control mice, but not in ATP2B1$^{+/-}$ mice, resulting in a similar contractile curve of control mice to that of ATP2B1$^{+/-}$ mice (85 ± 6 versus $91\pm10\%$; Fig. 5b). During constriction to the phenylephrine, vasorelaxation to acetylcholine in ATP2B1$^{+/-}$ vascular rings was significantly attenuated compared with that of control mice (45 ± 12 versus $86\pm8\%$; $P<0.05$; Fig. 5c), whereas the response to nitroprusside in ATP2B1$^{+/-}$ vascular rings was equivalent to that of control mice (78 ± 6 versus $87\pm4\%$; Fig. 5d).

Associations between nitric oxide production and blood pressure in ATP2B1$^{+/-}$ mice

In order to determine whether nitric oxide contributes to the blood pressure phenotype, we studied the expression and phosphorylation (Ser-1177) of eNOS in endothelial cells from ATP2B1$^{+/-}$ mice and control mice. The phosphorylation (Ser-1177) level of eNOS protein in ATP2B1$^{+/-}$ endothelial cells was significantly lower than that in control mice (Fig. 6a, b). In contrast, nNOS expression in VSMCs was not significantly different between the two groups (Fig. 6c, d). We also examined nitric oxide production in endothelial cells and aorta. NOx production in endothelial cells from ATP2B1$^{+/-}$ mice tended to be low than that from control mice (0.50 ± 0.25 versus 1.54 ± 0.43; $P=0.063$; Fig. 6e), and NOx production in aorta from ATP2B1$^{+/-}$ mice was significantly lower than that from control mice

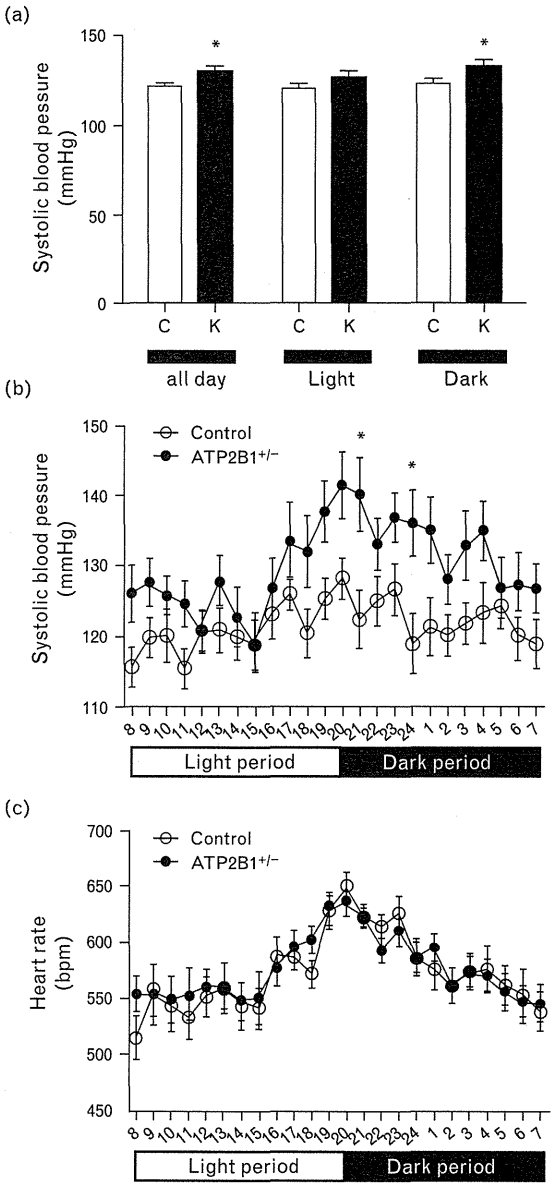

FIGURE 2 SBP and heart rate in ATP2B1$^{+/-}$ mice and control mice measured by radiotelemetric method. (a) Mean SBP of ATP2B1$^{+/-}$ mice and control mice during the entire days, light periods and dark periods. (b) Circadian patterns of SBP in ATP2B1$^{+/-}$ mice and control mice on a 12-h light (0800 to 2000 h)/dark (2000 to 0800 h) cycle. (c) Circadian patterns of heart rate in ATP2B1$^{+/-}$ mice and control mice on a 12-h light (0800 to 2000 h/dark (2000 to 0800 h) cycle. Mice were studied on a normal-salt diet. Values plotted are hourly means ($n = 12$ for each group). *$P < 0.05$ versus the control group. C, control mice; K, ATP2B1$^{+/-}$ mice.

(3.32 ± 0.16 versus 4.49 ± 0.21; $P < 0.01$; Fig. 6f) in basal conditions.

DISCUSSION

The study examined the relationships between ATP2B1 and hypertension using systemic heterozygous deletion mice. We demonstrated that ATP2B1$^{+/-}$ mice had higher blood pressure than genetic control mice under resting conditions, and found that the mechanisms of hypertension were partially due to impaired nitric oxide production in

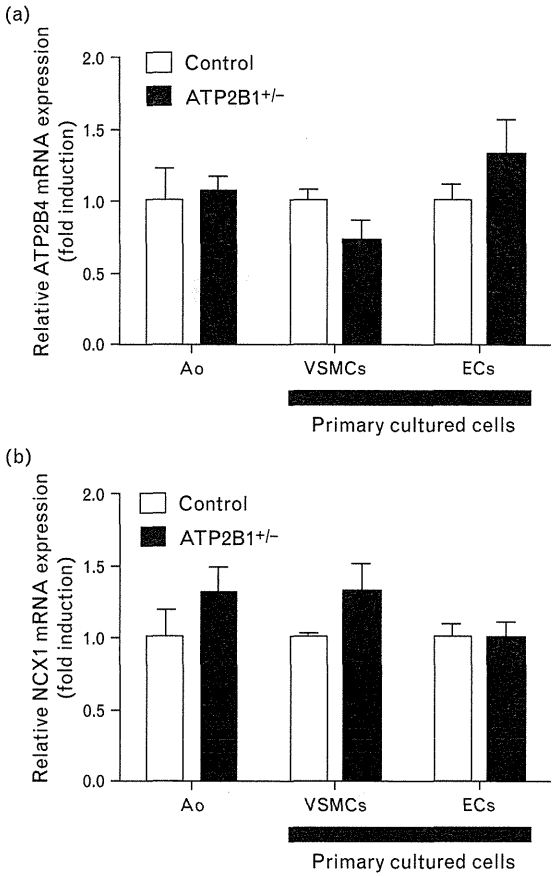

FIGURE 3 qRT-PCR measurement of ATP2B4 and NCX1 mRNA expression in aorta and isolated cells from ATP2B1$^{+/-}$ mice and control mice. (a) ATP2B4 mRNA expression in aorta and primary cultured cells quantified by qRT-PCR. (b) NCX1 mRNA expression in aorta and primary cultured cells quantified by qRT-PCR ($n = 6$ for each group). Ao, aorta; ECs, endothelial cells; qRT-PCR, quantitative reverse transcription-PCR; VSMCs, vascular smooth muscle cells.

vascular tissue. These results clarified that the ATP2B1 gene plays a crucial role in the regulation of blood pressure in the whole body. Recently, Shin *et al.* [25] published that silencing of ATP2B1 using siRNA increases blood pressure through vasoconstriction. These findings support our results that systemic heterozygous ATP2B1 null mice might cause blood pressure elevation.

Alterations of calcium-related genes in ATP2B1$^{+/-}$ mice

Although phenylephrine-induced intracellular calcium concentration was higher in ATP2B1$^{+/-}$ VSMCs than that in control VSMCs, gene expression of ATP2B4 and NCX1 was not altered. These results are congruent with those reported by Liu *et al.* [26], who demonstrated that ATP2B1$^{+/-}$ mice show no difference in basal intracellular calcium concentration in bladder smooth muscle compared with wild-type mice. On the contrary, after KCl stimulation, the bladder from ATP2B1$^{+/-}$ mice exhibited higher calcium concentration and force responses than the wild-type bladder [27]. We have already identified that mice with knockout of ATP2B1 in VSMCs showed blood pressure elevation due to increased intracellular calcium concentration and augmented vascular contractility [13].

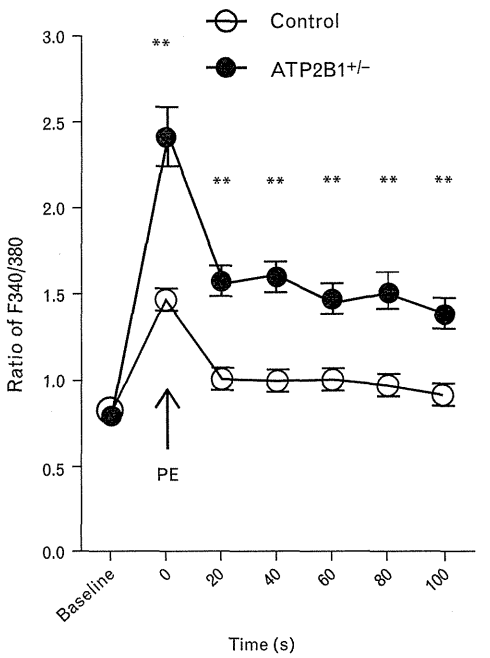

FIGURE 4 Calcium transient in primary cultured VSMCs from ATP2B1$^{+/-}$ mice and control mice. Measurement of basal conditions and PE-induced increase in intracellular calcium concentration of VSMCs were performed. Figure shows the time course of phenylephrine-stimulated change in intracellular calcium concentration in ATP2B1$^{+/-}$ VSMCs and control VSMCs. Data are displayed as ratio of F340/F380. Intracellular calcium concentration values over the entire cell were averaged to obtain the changes in the whole-cell calcium concentration ($n = 35–55$ cells for each group). $^{**}P < 0.01$ versus the control group. PE, phenylephrine; VSMCs, vascular smooth muscle cells.

We considered that the reason for unchanged NCX1 and ATP2B4 expression is due to the partial knockout of ATP2B1, and the rise in calcium concentration may be mild and influence blood pressure slightly in ATP2B1$^{+/-}$ mice.

Association between ATP2B1 and vasoconstriction

To clarify the mechanisms of hypertension in ATP2B1$^{+/-}$ mice, we measured isometric tension of vascular rings. Then we confirmed an increased contractile response to phenylephrine in vascular rings from ATP2B1$^{+/-}$ mice. Since phenylephrine activates inositol 1,4,5-triphosphate-induced intracellular calcium release and also stimulates voltage-independent calcium-permeable channels [28], the increased contractile response may be caused by alteration of intracellular calcium homeostasis; that is, ATP2B1$^{+/-}$ mice may have increased intracellular calcium concentration in VSMCs. On the contrary, we examined the effects of L-NAME (a NOS inhibitor) on vasoconstriction. In the presence of L-NAME, phenylephrine increased contractile ability in control mice, but not in ATP2B1$^{+/-}$ mice, and the contractile curve of control mice became similar to that of ATP2B1$^{+/-}$ mice. Furthermore, we confirmed the vasorelaxation to acetylcholine, but not to nitroprusside, was impaired in ATP2B1$^{+/-}$ mice. This finding supports that reduced ATP2B1 gene expression in the whole body may be associated with not only intracellular calcium concentration but also impaired eNOS activity and nitric oxide production.

Mechanisms of hypertension in ATP2B1$^{+/-}$ mice

We hypothesized two mechanisms of elevated blood pressure in this study. First, alteration of intracellular calcium homeostasis is a possible reason for hypertension. We reported previously that mice with ATP2B1 knockout in VSMCs showed increased blood pressure and intracellular calcium concentration [13]. Similarly, ATP2B1$^{+/-}$ mice also exhibited increased intracellular calcium concentration in VSMCs. However, vasoconstrictions in ATP2B1$^{+/-}$ mice were similar to that in control mice in the presence of L-NAME. In other words, if increased intracellular calcium concentration in ATP2B1$^{+/-}$ VSMCs is directly associated with the difference in contractile response, it is expected that phenylephrine-induced contraction in ATP2B1$^{+/-}$ vascular rings would remain augmented in the presence of L-NAME. Therefore, we concluded that the increases of contractile response are not mainly due to increased intracellular calcium concentration in VSMCs. Secondly, alteration of nitric oxide production is a possible reason for hypertension. Phenylephrine-induced contraction of ATP2B1$^{+/-}$ vascular rings did not differ in the absence or presence of L-NAME. This finding suggests that nitric oxide production is reduced in ATP2B1$^{+/-}$ endothelial cells. In order to determine whether eNOS contributes to nitric oxide production in ATP2B1$^{+/-}$ mice, we examined its expression and phosphorylation (Ser-1177) in endothelial cells from ATP2B1$^{+/-}$ and control mice. Phosphorylation of eNOS at Ser-1177 has been shown to increase its activity, whereas phosphorylation at Thr-495 is inhibitory, which seems to be particularly important in regulating eNOS activity [29–31]. The phosphorylation (Ser-1177) level of eNOS protein in ATP2B1$^{+/-}$ endothelial cells was significantly lower than that in control mice. On the contrary, nNOS expression in the aorta and VSMCs was not significantly different between the two groups. We also evaluated nitric oxide production in endothelial cells and aorta. Nitric oxide productions in endothelial cells and aorta from ATP2B1$^{+/-}$ mice were lower than that from control mice. Thus, the decreased nitric oxide productions in ATP2B1$^{+/-}$ endothelial cells were caused by impairment of the eNOS system, but not the nNOS system *in vivo* and *in vitro*. Several reports are available on animal models of hypertension induced by impaired nitric oxide production in endothelial cells, such as fructose-fed hypertensive rats [32], deoxycorticosterone acetate-salt hypertensive rats [33,34] and eNOS knockout mice [35,36]. In this way, impaired nitric oxide production in endothelial cells is commonly recognized as a cause of hypertension, and these experimental findings lead us to conclude that a partial mechanism of hypertension in ATP2B1$^{+/-}$ mice is associated with nitric oxide production.

Holton *et al.* [15] reported that eNOS activity is negatively regulated via interaction with PMCA2 and PMCA4, and expression of PMCA2 and PMCA4 in human umbilical vein endothelial cells (HUVEC) leads to decreased nitric oxide production. Although they showed PMCA1 interacts with eNOS in HUVEC using immunoprecipitation techniques, it has not been clarified whether PMCA1 modulates eNOS activity and nitric oxide production. Our data suggest that reduced expression of PMCA1 is associated with decreased nitric oxide production. As PMCA4 overexpression in VSMCs

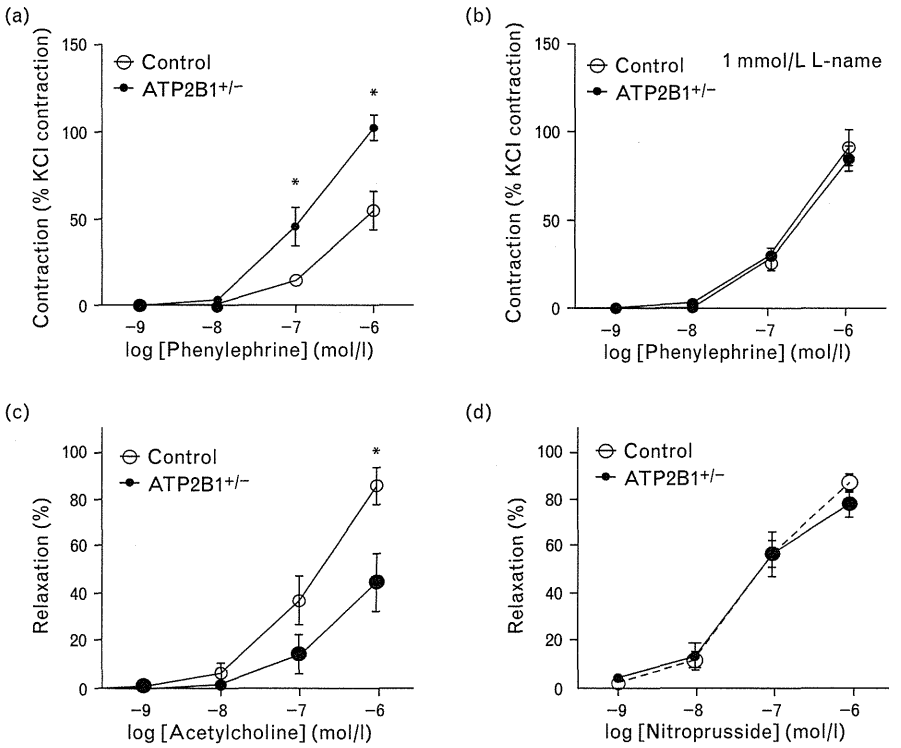

FIGURE 5 Vasoconstriction and vasorelaxation of vascular rings. Isolated vascular rings obtained from ATP2B1$^{+/-}$ mice and control mice were stimulated with phenylephrine. (a) Summary of phenylephrine concentration response curve. (b) Summary of phenylephrine concentration response curve in presence of 1 mmol/l L-NAME. Force is expressed as the percentage of the maximal contraction obtained in potassium-enriched solution ($n = 13$ for each group). Isolated vascular rings obtained from ATP2B1$^{+/-}$ mice and control mice were stimulated with acetylcholine or sodium nitroprusside during constriction to the phenylephrine. (c) Summary of acetylcholine concentration response curve. (d) Summary of nitroprusside concentration response curve. For relaxation response curves, forces were normalized as percentage of precontraction values ($n = 6$ for each group). *$P < 0.05$ versus the control group. L-NAME, $N\omega$-nitro-L-arginine methyl ester.

of mice has been reported to increase vascular reactivity and blood pressure with reduction of nNOS activity in VSMCs [16,17], the functions of PMCA1 and PMCA4 might be the reverse of each other with regard to vascular tone. In the present study, nNOS and PMCA4 expression did not differ in ATP2B1$^{+/-}$ mice. Thus, it is likely that elevated blood pressure is unrelated to the nNOS system in ATP2B1$^{+/-}$ mice.

Limitations

Firstly, as systemically ATP2B1 knockout mice are reported to be embryo-lethal, we adopted heterozygous ATP2B1 null mice to clarify the implication of ATP2B1 in blood pressure regulation. Secondly, we demonstrated that alteration of the eNOS system is associated with elevated blood pressure in ATP2B1$^{+/-}$ mice. However, decreased ATP2B1 gene expression was not limited to endothelial cells in these mice, so we cannot rule out the possibility of other mechanisms other than endothelium and VSMCs. It is obvious that ATP2B1 gene expression is associated with intracellular calcium concentration. If factors such as body fluid volume or vascular tone are changed by intracellular calcium regulation, they could affect blood pressure. Therefore, we need further investigation using other types of tissue-specific ATP2B1 knockout mice, and to elucidate the role of ATP2B1 in cells other than endothelial cells and VSMCs. Thirdly, molecular interactions between PMCA1 and the nitric oxide production pathway have not been fully understood. Further studies are needed to clarify the cause of down-regulation of eNOS activity in ATP2B1$^{+/-}$ mice. Fourthly, as the heart weight/body weight ratios were increased in ATP2B1$^{+/-}$ mice, the eNOS activity and nitric oxide production may be partially influenced by high blood pressure in itself. It is a future problem to clarify the functions and regulation mechanisms of PMCA1 in endothelium.

In conclusion, we generated ATP2B1$^{+/-}$ mice and confirmed the reduced ATP2B1 gene expression in the whole body. These mice showed not only enhanced vasoconstriction and elevated blood pressure but also impaired nitric oxide production by vascular tissue. Elevated blood pressure induced by decreased ATP2B1 gene expression may be associated with impaired eNOS activity and nitric oxide production.

ACKNOWLEDGEMENTS

We thank Dr Mika Kobayashi and Dr Tatsuhiko Kodama for support in isolating mouse aortic endothelial cells.

This work was supported by Grants for Scientific Research from the Ministry of Education, Culture, Sports, Science, and Technology, Japan; a Grant for a Science and Technology Incubation Program in Advanced Regions from the Japan Science and Technology Agency, Japan; Grants for Research from Yokohama City University, Japan and a Research Grant from Olympus Corporation.

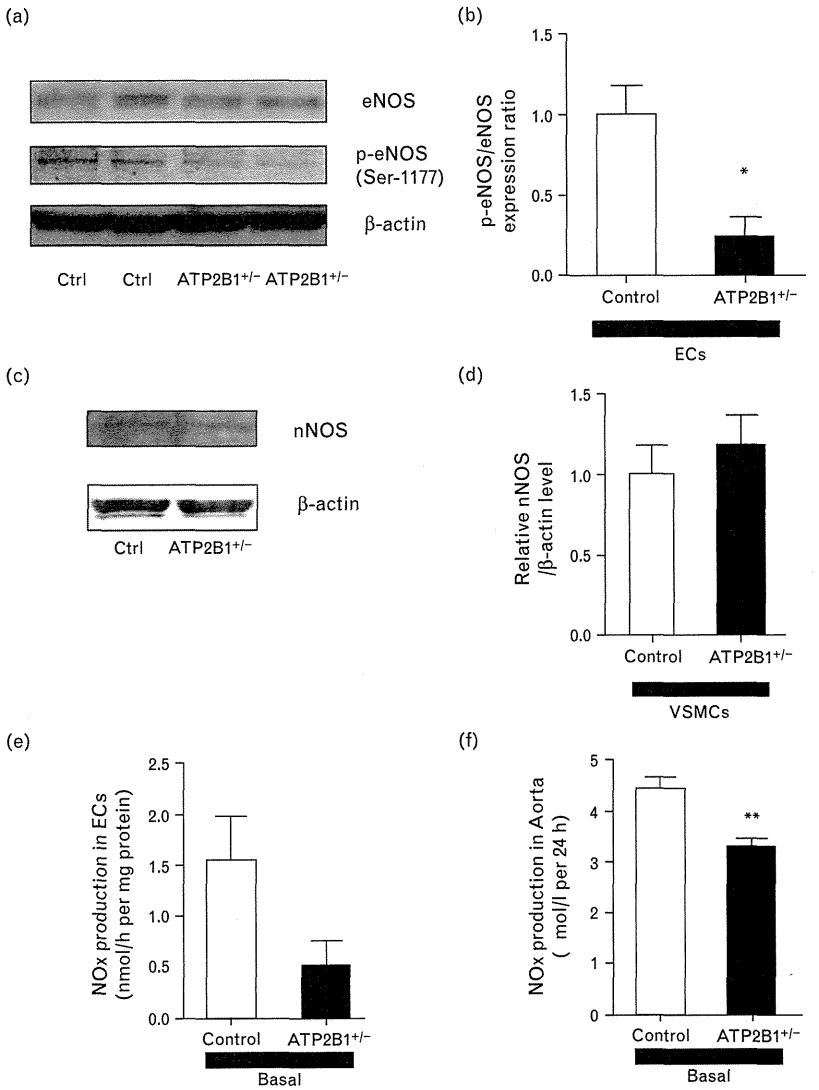

FIGURE 6 Nitric oxide synthase expression and NO production of ATP2B1$^{+/-}$ mice and control mice. (a) and (b) Representative western blot and quantitative analysis of phosphorylated eNOS (p-eNOS; Ser-1177), total eNOS and β-actin protein expression in ECs. Values are calculated as phosphorylated eNOS expression relative to total eNOS expression ($n=3$ for each group). (c) and (d) Representative western blot and quantitative analysis of nNOS and β-actin protein expression in VSMCs. Values are calculated as nNOS expression relative to β-actin expression ($n=4$ in each group). (e) and (f) NO production in ECs and aorta evaluated by measuring NOx by the Griess method. ECs and aorta were incubated for 24 h under basal conditions ($n=6$–11 for each group).*$P<0.05$ versus the control group. **$P<0.01$ versus the control group. ECs, endothelial cells; eNOS, endothelial nitric oxide synthase; NO, nitric oxide; NOx, nitrate/nitrite; VSMCs, vascular smooth muscle cells.

Conflicts of interest

Several authors (N.H., Y.T., H.U., T.M. and S.U.) have been named as the inventor on a patent application by Ehime University, Shiga University of Medical Science and Yokohama City University in work related to this study.

REFERENCES

1. Kearney PM, Whelton M, Reynolds K, Muntner P, Whelton PK, He J. Global burden of hypertension: analysis of worldwide data. *Lancet* 2005; 365:217–223.
2. Marteau JB, Zaiou M, Siest G, Visvikis-Siest S. Genetic determinants of blood pressure regulation. *J Hypertens* 2005; 23:2127–2143.
3. Tanira MO, Al Balushi KA. Genetic variations related to hypertension: a review. *J Hum Hypertens* 2005; 19:7–19.
4. Kohara K, Tabara Y, Nakura J, Imai Y, Ohkubo T, Hata A, *et al.* Identification of hypertension-susceptibility genes and pathways by a systemic multiple candidate gene approach: the Millennium Genome Project for Hypertension. *Hypertens Res* 2008; 31:203–212.
5. Levy D, Ehret GB, Rice K, Verwoert GC, Launer LJ, Dehghan A, *et al.* Genome-wide association study of blood pressure and hypertension. *Nat Genet* 2009; 41:677–687.
6. Cho YS, Go MJ, Kim YJ, Heo JY, Oh JH, Ban HJ, *et al.* A large-scale genome-wide association study of Asian populations uncovers genetic factors influencing eight quantitative traits. *Nat Genet* 2009; 41:527–534.
7. Takeuchi F, Isono M, Katsuya T, Yamamoto K, Yokota M, Sugiyama T, *et al.* Blood pressure and hypertension are associated with 7 loci in the Japanese population. *Circulation* 2010; 121:2302–2309.
8. Ehret GB, Munroe PB, Rice KM, Bochud M, Johnson AD, Chasman DI, *et al.* Genetic variants in novel pathways influence blood pressure and cardiovascular disease risk. *Nature* 2011; 478:103–109.
9. Carafoli E. Biogenesis: plasma membrane calcium ATPase: 15 years of work on the purified enzyme. *FASEB J* 1994; 8:993–1002.

10. Guerini D, Pan B, Carafoli E. Expression, purification, and characterization of isoform 1 of the plasma membrane Ca2+ pump: focus on calpain sensitivity. *J Biol Chem* 2003; 278:38141–38148.
11. Strehler EE, Zacharias DA. Role of alternative splicing in generating isoform diversity among plasma membrane calcium pumps. *Physiol Rev* 2001; 81:21–50.
12. Okunade GW, Miller ML, Pyne GJ, Sutliff RL, O'Connor KT, Neumann JC, *et al.* Targeted ablation of plasma membrane Ca2+-ATPase (PMCA) 1 and 4 indicates a major housekeeping function for PMCA1 and a critical role in hyperactivated sperm motility and male fertility for PMCA4. *J Biol Chem* 2004; 279:33742–33750.
13. Kobayashi Y, Hirawa N, Tabara Y, Muraoka H, Fujita M, Miyazaki N, *et al.* Mice lacking hypertension candidate gene ATP2B1 in vascular smooth muscle cells show significant blood pressure elevation. *Hypertension* 2012; 59:854–860.
14. Hirawa N, Fujiwara A, Umemura S. ATP2B1 and blood pressure: from associations to pathophysiology. *Curr Opin Nephrol Hypertens* 2013; 22:177–184.
15. Holton M, Mohamed TM, Oceandy D, Wang W, Lamas S, Emerson M, *et al.* Endothelial nitric oxide synthase activity is inhibited by the plasma membrane calcium ATPase in human endothelial cells. *Cardiovasc Res* 2010; 87:440–448.
16. Gros R, Afroze T, You XM, Kabir G, Van Wert R, Kalair W, *et al.* Plasma membrane calcium ATPase overexpression in arterial smooth muscle increases vasomotor responsiveness and blood pressure. *Circ Res* 2003; 93:614–621.
17. Schuh K, Quaschning T, Knauer S, Hu K, Kocak S, Roethlein N, *et al.* Regulation of vascular tone in animals overexpressing the sarcolemmal calcium pump. *J Biol Chem* 2003; 278:41246–41252.
18. de Lange WJ, Halabi CM, Beyer AM, Sigmund CD. Germ line activation of the Tie2 and SMMHC promoters causes noncell-specific deletion of floxed alleles. *Physiol Genomics* 2008; 35:1–4.
19. Kisanuki YY, Hammer RE, Miyazaki J, Williams SC, Richardson JA, Yanagisawa M. Tie2-Cre transgenic mice: a new model for endothelial cell-lineage analysis in vivo. *Dev Biol* 2001; 230:230–242.
20. Kobayashi M, Inoue K, Warabi E, Minami T, Kodama T. A simple method of isolating mouse aortic endothelial cells. *J Atheroscler Thromb* 2005; 12:138–142.
21. Sakai M, Tamura K, Tsurumi Y, Tanaka Y, Koide Y, Matsuda M, *et al.* Expression of MAK-V/Hunk in renal distal tubules and its possible involvement in proliferative suppression. *Am J Physiol Renal Physiol* 2007; 292:F1526–F1536.
22. Mills PA, Huetteman DA, Brockway BP, Zwiers LM, Gelsema AJM, Schwartz RS, *et al.* A new method for measurement of blood pressure, heart rate, and activity in the mouse by radiotelemetry. *J Appl Physiol* 2000; 88:1537–1544.
23. Akaike T, Jin MH, Yokoyama U, Izumi-Nakaseko H, Jiao Q, Iwasaki S, *et al.* T-type Ca2+ channels promote oxygenation-induced closure of the rat ductus arteriosus not only by vasoconstriction but also by neointima formation. *J Biol Chem* 2009; 284:24025–24034.
24. Markewitz BA, Michael JR, Kohan DE. Cytokine-induced expression of a nitric oxide synthase in rat renal tubule cells. *J Clin Invest* 1993; 91:2138–2143.
25. Shin YB, Lim JE, Ji SM, Lee HJ, Park SY, Hong KW, *et al.* Silencing of Atp2b1 increases blood pressure through vasoconstriction. *J Hypertens* 2013; 31:1575–1583.
26. Liu L, Ishida Y, Okunade G, Shull GE, Paul RJ. Role of plasma membrane Ca2+-ATPase in contraction-relaxation processes of the bladder: evidence from PMCA gene-ablated mice. *Am J Physiol Cell Physiol* 2006; 290:C1239–C1247.
27. Liu L, Ishida Y, Okunade G, Pyne-Geithman GJ, Shull GE, Paul RJ. Distinct roles of PMCA isoforms in Ca2+ homeostasis of bladder smooth muscle: evidence from PMCA gene-ablated mice. *Am J Physiol Cell Physiol* 2007; 292:C423–C431.
28. McDaniel SS, Platoshyn O, Wang J, Yu Y, Sweeney M, Krick S, *et al.* Capacitative Ca(2+) entry in agonist-induced pulmonary vasoconstriction. *Am J Physiol Lung Cell Mol Physiol* 2001; 280:L870–L880.
29. Dudzinski DM, Michel T. Life history of eNOS: partners and pathways. *Cardiovasc Res* 2007; 75:247–260.
30. Fleming I, Busse R. Molecular mechanisms involved in the regulation of the endothelial nitric oxide synthase. *Am J Physiol Regul Integr Comp Physiol* 2003; 284:R1–R12.
31. Dimmeler S, Fleming I, Fisslthaler B, Hermann C, Busse R, Zeiher AM. Activation of nitric oxide synthase in endothelial cells by Akt-dependent phosphorylation. *Nature* 1999; 399:601–605.
32. Tran LT, Yuen VG, McNeill JH. The fructose-fed rat: a review on the mechanisms of fructose-induced insulin resistance and hypertension. *Mol Cell Biochem* 2009; 332:145–159.
33. Kirchner KA, Scanlon PH Jr, Dzielak DJ, Hester RL. Endothelium-derived relaxing factor responses in Doca-salt hypertensive rats. *Am J Physiol* 1993; 265:R568–R572.
34. Schiffrin EL. Vascular endothelin in hypertension. *Vascul Pharmacol* 2005; 43:19–29.
35. Shesely EG, Maeda N, Kim HS, Desai KM, Krege JH, Laubach VE, *et al.* Elevated blood pressures in mice lacking endothelial nitric oxide synthase. *Proc Natl Acad Sci U S A* 1996; 93:13176–13181.
36. Huang PL, Huang Z, Mashimo H, Bloch KD, Moskowitz MA, Bevan JA, *et al.* Hypertension in mice lacking the gene for endothelial nitric oxide synthase. *Nature* 1995; 377:239–242.

Reviewers' Summary Evaluations

Referee 1

This study by Fujiwara and colleagues provides evidence of the functional consequences of reduced expression of ATP2B1/PMCA1 and further validates GWAS data that ATP2B1 is associated with the regulation of blood pressure. Whilst the study revealed that NO production by eNOS was impaired the exact mechanistic association between PMCA1 and eNOS remains to be addressed. The authors largely restricted their analyses to the vasculature and did not investigate the effect of deletion of ATP2B1 on other tissues that are important in the regulation of and influenced by blood pressure even though a model carrying a systemic heterozygous mutation was generated.

Referee 2

ATP2B1 gene, which codes the plasma membrane calcium ATPase isoform 1 (PMCA1), is a candidate gene for high blood pressure. However, evidences supporting such hypothesis are scant, and the mechanisms by which ATP2B1 gene could regulate blood pressure are unknown. Fujiwara and coll., by using a model created in their lab, i.e. the heterozygous ATP2B1 null (ATP2B1+/−) mice, showed that reduced ATP2B1 gene is associated with high blood pressure, reduced NO production and blunted vasorelaxation to acetylcholine. Hence, this study first identified NO production as the mechanism underlying deficient ATP2B1-induced hypertension.

OPEN

Deletion of the angiotensin II type 1 receptor–associated protein enhances renal sodium reabsorption and exacerbates angiotensin II–mediated hypertension

Masato Ohsawa[1], Kouichi Tamura[1], Hiromichi Wakui[1], Akinobu Maeda[1], Toru Dejima[1], Tomohiko Kanaoka[1], Kengo Azushima[1], Kazushi Uneda[1], Yuko Tsurumi-Ikeya[1], Ryu Kobayashi[1], Miyuki Matsuda[1], Shinichi Uchida[2], Yoshiyuki Toya[1], Hiroyuki Kobori[3], Akira Nishiyama[3], Akio Yamashita[4], Yoshihiro Ishikawa[5] and Satoshi Umemura[1]

[1]Department of Medical Science and Cardiorenal Medicine, Yokohama City University Graduate School of Medicine, Yokohama, Japan; [2]Department of Nephrology, Graduate School of Medicine, Tokyo Medical and Dental University, Tokyo, Japan; [3]Department of Pharmacology, Kagawa University School of Medicine, Kagawa, Japan; [4]Department of Molecular Biology, Yokohama City University Graduate School of Medicine, Yokohama, Japan and [5]Cardiovascular Research Institute, Yokohama City University Graduate School of Medicine, Yokohama, Japan

Angiotensin II type 1 receptor (AT1R)–associated protein (ATRAP) promotes AT1R internalization along with suppression of pathological activation of tissue AT1R signaling. However, the functional significance of ATRAP in renal sodium handling and blood pressure regulation under pathological stimuli is not fully resolved. Here we show the blood pressure of mice with a gene-targeted disruption of ATRAP was comparable to that of wild-type mice at baseline. However, in ATRAP-knockout mice, angiotensin II–induced hypertension was exacerbated and the extent of positive sodium balance was increased by angiotensin II. Renal expression of the sodium-proton antiporter 3, a major sodium transporter in the proximal tubules, urinary pH, renal angiotensinogen production, and angiotensin II content was unaffected. Stimulation of the renal expression and activity of the epithelial sodium channel (ENaC), a major sodium transporter in the distal tubules, was significantly enhanced by chronic angiotensin II infusion. The circulating and urinary aldosterone levels were comparable. The blood pressure response and renal ENaC expression by aldosterone were not affected. Thus, ATRAP deficiency exacerbated angiotensin II–mediated hypertension by pathological activation of renal tubular AT1R by angiotensin II. This directly stimulates ENaC in the distal tubules and enhances sodium retention in an aldosterone-independent manner.

Correspondence: *Kouichi Tamura, Department of Medical Science and Cardiorenal Medicine, Yokohama City University Graduate School of Medicine, 3-9 Fukuura, Kanazawa-ku, Yokohama 236-0004, Japan. E-mail: tamukou@med.yokohama-cu.ac.jp*

Received 2 May 2013; revised 7 February 2014; accepted 13 February 2014; published online 2 April 2014

Kidney International (2014) **86,** 570–581; doi:10.1038/ki.2014.95; published online 2 April 2014

KEYWORDS: angiotensin; blood pressure; cell signaling; epithelial sodium transport; hypertension; renin–angiotensin system

Hypertension is the most common chronic disease worldwide. It has a complex etiology in which genetic and environmental factors are intricately intertwined. Although the mechanisms underlying hypertension are difficult to fully elucidate, the renin–angiotensin system (RAS) has a pivotal role in it. Among tissue RAS forms, activation of angiotensin II type 1 receptor (AT1R) signaling in the renal tubules is suggested to have a key role in altered renal sodium handling that occurs in hypertension. According to Guyton's hypothesis, it is maintained that hypertension is caused by a disproportionate suppression of sodium excretion from kidney due to arterial pressure.[1] Therefore, pathological activation of renal tubule AT1R signaling provokes defective renal sodium handling, with a consequent dysregulation of body fluid volume that, in turn, leads to development of hypertension.

The AT1R-associated protein (ATRAP/*Agtrap*) has been identified as a specific AT1R-binding protein.[2,3] Previous studies have shown that ATRAP selectively suppresses angiotensin II (Ang II)–mediated pathological activation of AT1R in cardiovascular cells, and that cardiac ATRAP enhancement ameliorates cardiac hypertrophy in Ang II–infused mice without any effect on baseline cardiovascular functions, including blood pressure (BP).[4–8] Based on these observations, we hypothesized that a downregulation of tissue ATRAP enhances pathological activation of tissue AT1R in response to certain stimuli without any evident effect on baseline physiological AT1R signaling. ATRAP is abundantly

distributed along the renal tubules.[9,10] Therefore, we investigated the effects of chronic Ang II infusion on BP and renal sodium handling in the context of gene-specific disruption of ATRAP (ATRAP-knockout (KO) mice).

RESULTS

ATRAP deficiency exerts no evident effect on renal morphology and function or AT1R expression

The ATRAP mRNA was widely distributed in the tissues of littermate wild-type control mice (WT mice) with the highest expression in kidney (Figure 1a). In contrast, no ATRAP expression was detected in any tissues, including the kidney, in ATRAP-KO mice (Figure 1a and b). On immunohistochemical analysis with consecutive sections using markers specific to the tubular segments, such as megalin (proximal convoluted tubules), calbindin-D (distal convoluted tubules and connecting tubules), and aquaporin 2 (collecting ducts), ATRAP immunostaining was broadly detected in nephron segments from proximal convoluted tubules to collecting ducts of WT mice (Figure 1c). In contrast, there was no ATRAP immunostaining in nephron segments of ATRAP-KO mice (Figure 1d). Although genetic inactivation of other RAS components, such as angiotensinogen (AGT), renin, and AT1R, has been reported to result in renal morphological

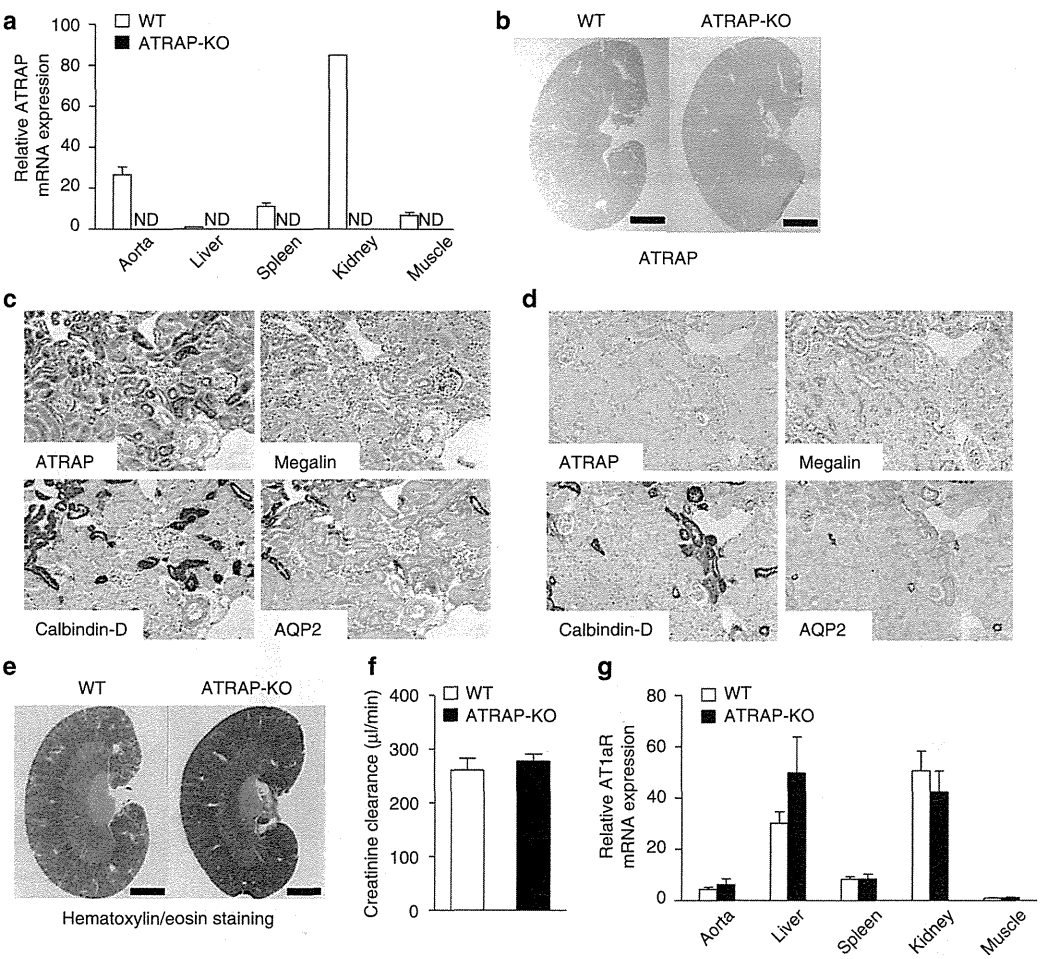

Figure 1 | Angiotensin II type 1 receptor (AT1R)-associated protein (ATRAP) deficiency exerts no evident effect on renal morphology or AT1R gene expression. (**a**) ATRAP mRNA is widely distributed in many different tissues and abundantly expressed in the kidney of wild-type (WT) mice. Values are calculated relative to those achieved with extracts from the liver of WT mice and are expressed as mean ± s.e. ($n = 2$ in each group). ND, not detected. (**b**) ATRAP protein is abundantly expressed in the kidney of WT mice on immunohistochemistry. The positive areas for ATRAP immunostaining are evident as brown dots in the sections. Scale bar = 1.5 mm. Original magnification ×40. (**c**) In WT mice, the ATRAP protein is expressed along the nephron segments from the proximal to distal tubules in consecutive renal cortical sections, as shown by immunohistochemistry. AQP2, aquaporin-2, a specific marker of the collecting ducts; Calbindin-D, a specific marker of distal convoluted tubules (DCTs) and connecting tubules (CNTs); Megalin, a specific marker of the proximal tubules. Original magnification ×200. (**d**) In ATRAP-knockout (KO) mice, there is no ATRAP immunostaining in the renal tubules. Original magnification ×200. (**e**) There is no anatomical difference between the kidneys of the WT and ATRAP-KO mice on representative hematoxylin/eosin staining of kidney sections. Scale bar = 1.5 mm. Original magnification ×40. (**f**) ATRAP deficiency does not affect the creatinine clearance. Values are expressed as mean ± s.e. ($n = 4$ in each group). (**g**) ATRAP deficiency does not affect the tissue distribution or expression levels of AT1R mRNA. The values were calculated relative to those achieved with extracts from the muscles of WT mice and are expressed as mean ± s.e. ($n = 4$–6 in each group).

alteration even under baseline conditions,[11–15] ATRAP-KO mice at baseline exhibited no apparent alterations in renal morphology (Figure 1e) or creatinine clearance (Figure 1f, 260.8 ± 21.7 in WT vs. 277.6 ± 13.2 in ATRAP-KO, μl/min, $P = 0.918$; unpaired t-test). Furthermore, there was no significant difference in AT1R mRNA expression between WT and ATRAP-KO mice (Figure 1g).

ATRAP deficiency exerts no apparent effect on baseline BP or urinary pH

Genetic deficiency of the RAS components (that is, AGT, renin, and AT1R) has also been reported to result in significant decreases in baseline BP.[11–15] However, baseline 24-h mean systolic BP, diastolic BP, and heart rate, measured by radiotelemetric method, were similar in WT and ATRAP-KO mice (Figure 2a, systolic BP 120 ± 2 vs. 123 ± 4, mm Hg, $P = 0.545$; Figure 2b, diastolic BP 92 ± 5 vs. 95 ± 4, mm Hg, $P = 0.793$; Figure 2c, HR 541 ± 18 vs. 547 ± 10 beat/min, $P = 0.598$; unpaired t-test). Urinary pH, which reflects the activity of sodium-proton antiporter 3 (NHE3), was also similar in WT and ATRAP-KO mice (Figure 2d).

ATRAP deficiency exacerbates Ang II-induced hypertension

As ATRAP-KO mice did not display any alternation in baseline BP, we next examined the effects of ATRAP deficiency on BP response to chronic Ang II infusion (500 or 2000 ng/kg/min). Whereas systolic BP was increased during the period of chronic Ang II infusion in WT mice, Ang II-induced elevation of systolic BP was significantly exacerbated in ATRAP-KO mice compared with WT mice, irrespective of dose (Figure 3a; Ang II, 500 ng/kg/min, $F = 6.117$, $P = 0.048$; Figure 3b, Ang II, 2000 ng/kg/min, $F = 86.758$,

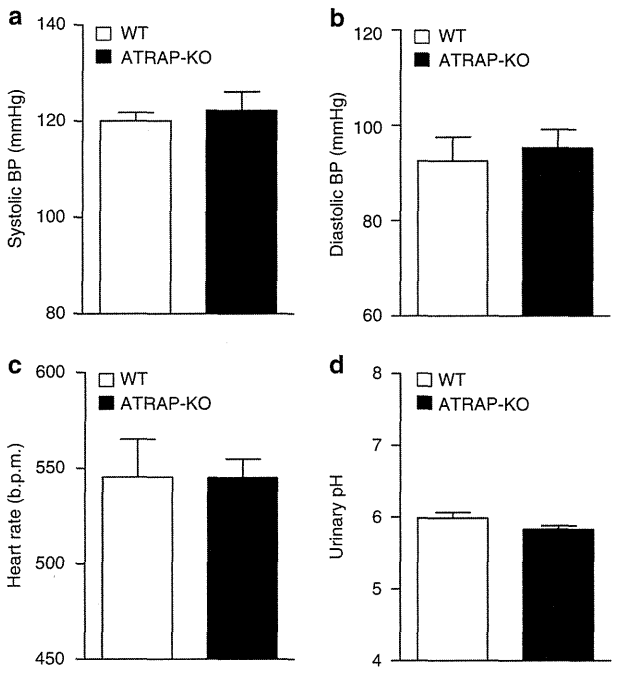

Figure 2 | Angiotensin II type 1 receptor (AT1R)-associated protein (ATRAP) deficiency exerts no apparent effect on baseline blood pressure (BP) or urinary pH. (**a**) Systolic BP, (**b**) diastolic BP, and (**c**) heart rate measured by a radiotelemetric method were similar in the wild-type (WT) and ATRAP-knockout (KO) mice. (**d**) Urinary pH was also comparable in the WT and ATRAP-KO mice. Values are expressed as mean ± s.e. ($n = 5$–6 in each group).

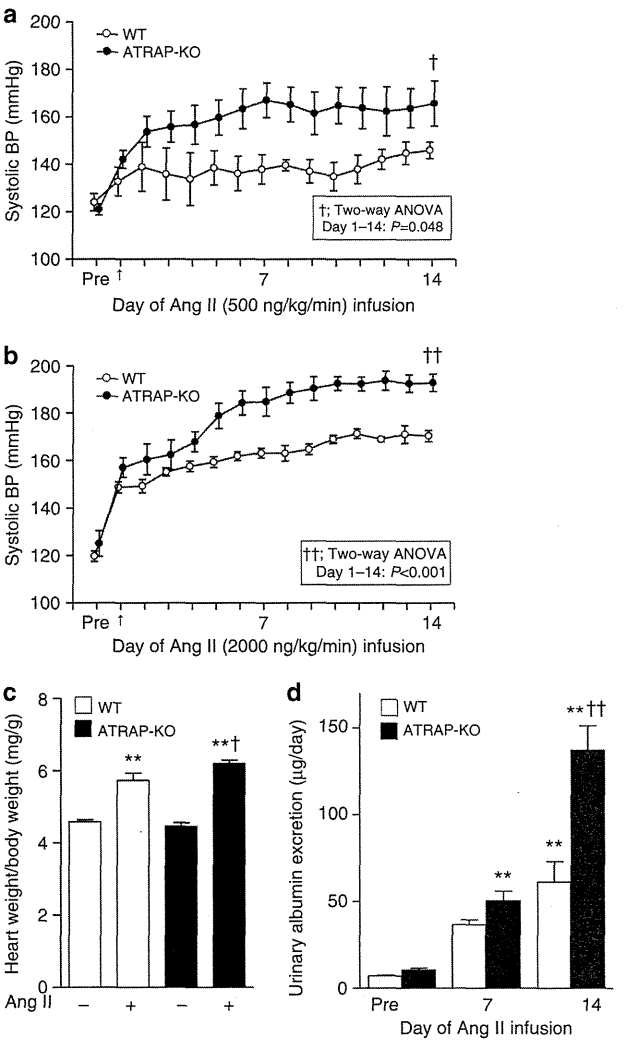

Figure 3 | Angiotensin II type 1 receptor (AT1R)-associated protein (ATRAP) deficiency exacerbates angiotensin II (Ang II)-mediated hypertension. The Ang II-induced elevation of systolic blood pressure (BP) was significantly exacerbated in ATRAP-knockout (KO) mice as compared with wild-type (WT) mice irrespective of the Ang II dose (**a**, 500 ng/kg/min; **b**, 2000 ng/kg/min). Values are expressed as mean ± s.e. ($n = 4$ in each group). $^{\dagger}P < 0.05$ versus WT mice, $^{\dagger\dagger}P < 0.01$ versus WT mice. (**c**) ATRAP-KO mice exhibited a significantly increased ratio of heart weight/body weight compared with WT mice after Ang II (2000 ng/kg/min) infusion. Values are expressed as mean ± s.e. ($n = 7$–9 in each group). $^{**}P < 0.01$ versus vehicle, $^{\dagger}P < 0.05$ versus WT mice. (**d**) Urinary albumin excretion was further elevated in ATRAP-KO mice compared with WT mice after Ang II (2000 ng/kg/min) infusion. Values are expressed as mean ± s.e. ($n = 6$–8 in each group). $^{**}P < 0.01$ versus vehicle, $^{\dagger\dagger}P < 0.01$ versus WT mice.

$P<0.001$, two-way repeated measures analysis of variance (ANOVA)). We employed a higher dose of Ang II (2000 ng/kg/min) for further experiments to characterize ATRAP-KO mice in comparison with WT mice.

The ATRAP-KO mice also exhibited a significantly increased ratio of heart weight/body weight compared with WT mice by Ang II (Figure 3c, $P=0.040$; analysis of variance (ANOVA). Similarly, urinary albumin excretion was elevated in ATRAP-KO mice compared with WT mice (Figure 3d; $P<0.001$. ANOVA). The mortality rate was comparable in WT and ATRAP-KO mice during Ang II infusion (2000 ng/kg/min) for 14 days (5.7 vs. 7.3%, $P=0.576$, χ^2-test).

ATRAP deficiency inhibits urinary sodium excretion during Ang II infusion

As the highest ATRAP expression was observed in renal tubules among analyzed tissues, we hypothesized that ATRAP deficiency might enhance Ang II–mediated hypertension by affecting renal sodium handling. To examine this, we performed metabolic cage analysis (Figure 4a–d). Day-by-day sodium intake was similar in WT and ATRAP-KO mice (Figure 4a, $F=0.559$, $P=0.469$, two-way repeated measures ANOVA), and urinary sodium excretion was comparable in WT and ATRAP-KO mice (Figure 4b, $F=1.690$, $P=0.218$, two-way repeated measures ANOVA). However, day-by-day sodium balance was significantly increased in ATRAP-KO mice compared with WT mice over the entire Ang II infusion period (Figure 4c, $F=4.892$, $P=0.047$, two-way repeated measures ANOVA). Furthermore, the extent of cumulative sodium balance during 14 days of Ang II infusion was significantly increased in ATRAP-KO mice as compared with WT mice (Figure 4d, $P=0.047$, unpaired t-test), consistent with blunted natriuresis as a mechanism for the exacerbation of Ang II-induced hypertension.

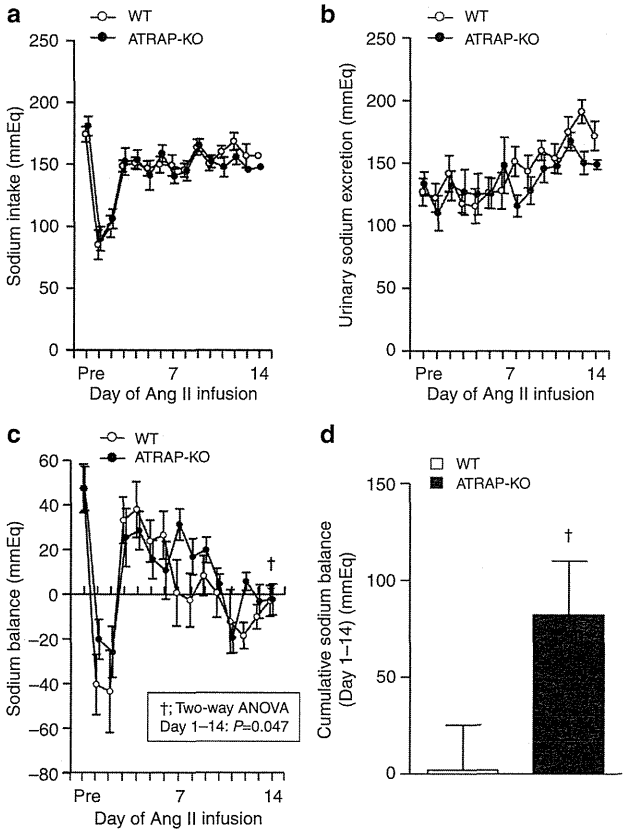

Figure 4 | Angiotensin II type 1 receptor (AT1R)–associated protein (ATRAP) deficiency exacerbates sodium retention during angiotensin II (Ang II) infusion. (**a**) Day-by-day sodium intake was comparable in the wild-type (WT) and ATRAP-knockout (KO) mice during the entire period of Ang II (2000 ng/kg/min) infusion ($F=0.559$, $P=0.469$, two-way repeated measures analysis of variance (ANOVA)). (**b**) Day-by-day urinary sodium excretion was comparable in the WT and ATRAP-KO mice during the entire period of Ang II infusion ($F=1.690$, $P=0.218$, two-way repeated measures ANOVA). (**c**) Day-by-day sodium balance was significantly increased in the ATRAP-KO mice compared with the WT mice for the whole period of Ang II infusion ($F=4.892$, $P=0.047$, two-way repeated measures ANOVA). (**d**) The extent of the cumulative positive sodium balance during the Ang II (2000 ng/kg/min) infusion period was significantly increased in the ATRAP-KO mice compared with the WT mice on metabolic cage analysis. Values are expressed as mean ± s.e. ($n=7$–8 in each group). $^{\dagger}P<0.05$ versus WT mice.

ATRAP deficiency enhances renal expression of α-subunit of the epithelial sodium channel (αENaC) by chronic Ang II infusion

To investigate the mechanisms involved in the suppression of urinary sodium excretion in response to Ang II in ATRAP-KO mice, we compared renal expression of major sodium transporters (NHE3, sodium–potassium–two chloride co-transporter (NKCC2), Na^+–Cl^- cotransporter (NCC), and ENaC subunits). Age-matched WT and ATRAP-KO mice were divided into four groups: (1) vehicle-infused WT mice, (2) Ang II–infused WT mice, (3) vehicle-infused ATRAP-KO mice, and (4) Ang II–infused ATRAP-KO mice. There were no differences in the expression levels of NHE3 or NKCC mRNA and protein between WT and ATRAP-KO mice with or without Ang II infusion for 14 days (Figures 5a and b and 6a and b). On the other hand, although Ang II–mediated increase in NCC mRNA was significant only in ATRAP-KO mice (Figure 5c), renal expression of phosphorylated NCC, which is the activated NCC protein, was similarly increased by Ang II infusion in both groups (Figure 6c).

However, Ang II–mediated upregulation of αENaC, but not of βENaC or γENaC mRNA, was significantly enhanced in ATRAP-KO mice compared with WT mice (Figure 5d–f). Furthermore, although αENaC protein expression did not differ between WT and ATRAP-KO mice with vehicle, there was a significant Ang II–mediated increase in renal αENaC protein expression in ATRAP-KO mice ($P=0.007$ relative to vehicle-infused ATRAP-KO mice, $P=0.042$ relative to Ang II–infused WT mice, ANOVA; Figure 6d). Protein levels of βENaC and γENaC were similar in WT and ATRAP-KO mice (Figure 6e and f).

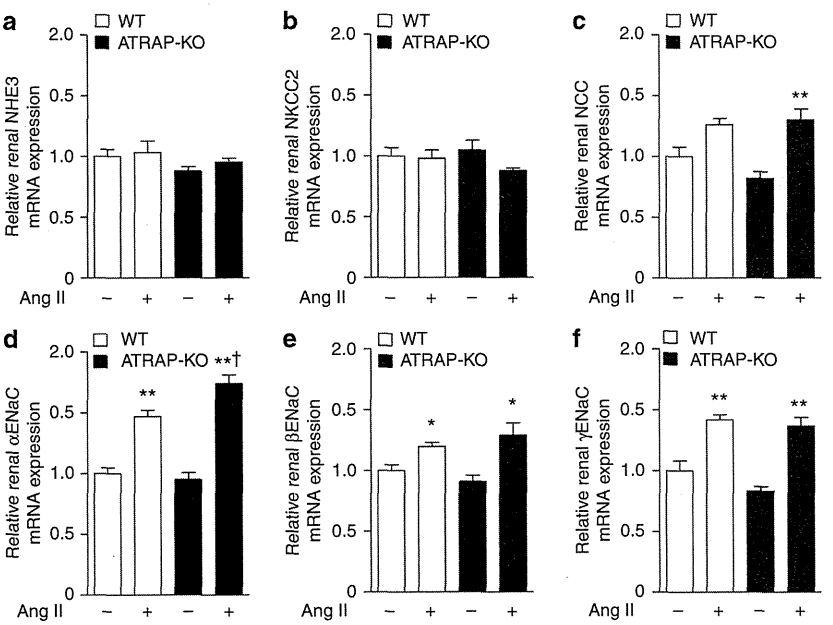

Figure 5 | Angiotensin II type 1 receptor (AT1R)-associated protein (ATRAP) deficiency enhances the upregulation of renal α-subunit of the epithelial sodium channel (αENaC) mRNA expression by chronic angiotensin II (Ang II) infusion. Effects of Ang II (2000 ng/kg/min) infusion for 14 days on the mRNA expression of the major sodium transporters (**a**, sodium-proton antiporter 3 (NHE3); **b**, sodium–potassium–two chloride cotransporter (NKCC2); **c**, Na^+–Cl^- cotransporter (NCC); **d**, αENaC; e, βENaC; and **f**, γENaC) in the kidneys of wild-type (WT) and ATRAP-knockout (KO) mice. Values are expressed as mean ± s.e. ($n = 6$–8 in each group). $^*P < 0.05$ versus vehicle, $^{**}P < 0.01$ versus vehicle, $^{\dagger}P < 0.05$ versus WT mice.

ATRAP deficiency–mediated enhancement of renal αENaC expression by chronic Ang II infusion is aldosterone independent

The promoting effect of Ang II infusion on expression of renal RAS components including AGT in proximal tubules has been reported.[16,17] Thus, to investigate the mechanisms involved in Ang II–induced renal αENaC expression in ATRAP-KO mice, renal AGT mRNA expression, urinary AGT excretion, and renal Ang II levels were analyzed. However, renal AGT mRNA expression and urinary AGT excretion were similar in WT and ATRAP-KO mice with vehicle, and exhibited no apparent changes by Ang II (Figure 7a and b). In addition, renal Ang II level was comparable in WT and ATRAP-KO mice with vehicle, and was significantly and similarly increased by Ang II in both WT and ATRAP-KO mice (Figure 7c). These results indicate that ATRAP deficiency exerts no apparent effect on proximal tubule AGT production or the renal Ang II levels.

We next examined the plasma aldosterone concentration and urinary aldosterone excretion to investigate a possible role of aldosterone in the enhanced αENaC expression in response to Ang II. Under vehicle infusion, plasma aldosterone concentration (Figure 8a, 208.7 ± 38.1 vs. 197.5 ± 29.3 pg/ml, $P = 1.000$, ANOVA) and urinary aldosterone excretion (Figure 8b, 5.2 ± 0.6 vs. 4.6 ± 0.8 ng/day, $P = 0.974$, ANOVA) were comparable in WT and ATRAP-KO mice. Furthermore, Ang II infusion significantly and similarly increased plasma aldosterone concentration (Figure 8a, 1154.0 ± 170.5 vs. 1464.5 ± 267.9 pg/ml, $P = 0.401$, ANOVA) and urinary aldosterone excretion (Figure 8b, 19.2 ± 0.5 vs. 15.9 ± 2.1 ng/day, $P = 0126$, ANOVA) in both WT and ATRAP-KO mice.

We also administered exogenous aldosterone subcutaneously to WT and ATRAP-KO mice. Systolic BP measured by the tail-cuff method was similar in WT and ATRAP-KO mice by vehicle administration, and was similarly increased by chronic aldosterone infusion in both groups (Figure 9a). Furthermore, renal αENaC protein levels did not exhibit any significant difference between WT and ATRAP-KO mice with or without aldosterone (Figure 9b). These results would support the notion that ATRAP deficiency enhances renal αENaC expression in an aldosterone-independent manner.

ENaC is functionally activated in response to chronic Ang II simulation and promotes renal sodium retention in ATRAP deficiency

To examine whether ENaC activity was affected by the enhancement of renal αENaC expression in ATRAP-KO mice, diuretic test using a potent and specific ENaC inhibitor amiloride was performed, and the effects of ATRAP deficiency on the functional transport activity of ENaC were examined. Urinary sodium excretion and urinary volume after intraperitoneal injection of amiloride were significantly increased in the Ang II–infused ATRAP-KO as mice

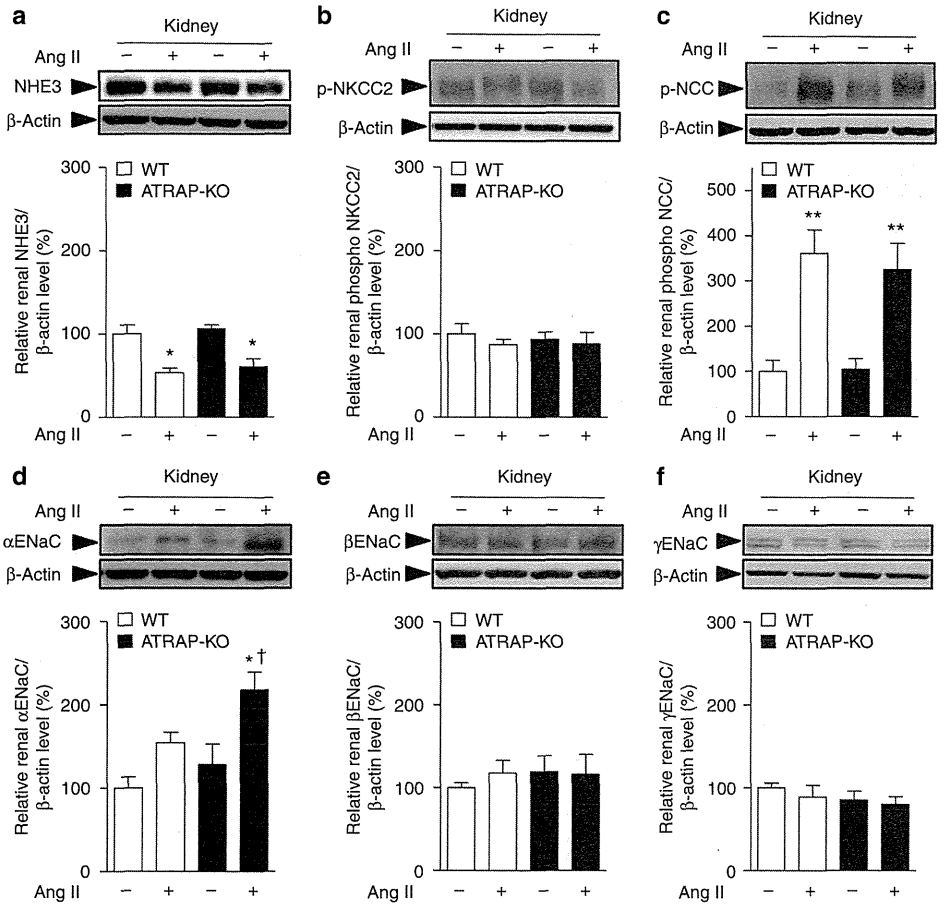

Figure 6 | Angiotensin II type 1 receptor (AT1R)-associated protein (ATRAP) deficiency enhances upregulation of renal α-subunit of the epithelial sodium channel (αENaC) protein expression by chronic angiotensin II (Ang II) infusion. Effects of Ang II (2000 ng/kg/min) infusion for 14 days on protein expression of the major sodium transporters (**a**, sodium-proton antiporter 3 (NHE3); **b**, phosphorylated sodium–potassium–two chloride cotransporter (NKCC2) on Thr96; **c**, phosphorylated Na^+–Cl^- cotransporter (NCC) on Ser71; **d**, αENaC; **e**, βENaC; and **f**, γENaC) in the kidneys of wild-type (WT) and ATRAP-knockout (KO) mice. Values are expressed as mean ± s.e. ($n = 6$–8 in each group). $^*P < 0.05$ versus vehicle, $^{**}P < 0.01$ versus vehicle, $^{\dagger}P < 0.05$ versus WT mice.

compared with the Ang II–infused WT mice (Figure 10a and b). This finding indicated that the ENaC is functionally activated in response to chronic Ang II simulation so as to increase renal sodium retention in ATRAP-KO mice.

ATRAP deficiency enhances Ang II–induced vasoconstriction

Although the renal αENaC protein expression in ATRAP-KO mice was significantly increased as compared with WT mice by chronic Ang II infusion for 14 days (Figure 6d), the αENaC protein expression levels just after the start of Ang II infusion (on day 1) did not differ significantly between WT and ATRAP-KO mice (Figure 11). On the other hand, telemetric BP showed a trend toward enhanced Ang II–induced BP elevation in ATRAP-KO mice, concomitant with a tendency of increase in day-by-day sodium balance in ATRAP-KO mice as compared with WT mice already during the early period of Ang II infusion (Figures 3 and 4).

Based on the above observations, we examined the vasoconstrictor response of artery rings to Ang II to investigate whether there would be an enhancement of vascular response to Ang II as one of the contributing factors to the exaggerated BP elevation in the initial phase of Ang II infusion in ATRAP-KO mice. Histological analysis of aortic sections revealed a normal vascular structure in ATRAP-KO mice, in spite of no vascular ATRAP immunostaining, without any alteration in aortic medial thickness in ATRAP-KO mice (Figure 12a and b). However, Ang II provoked an exaggerated vasoconstrictor response of vascular rings of ATRAP-KO mice compared with WT mice upon vessel wire myograph analysis (Figure 12c, $F = 8.583$, $P = 0.015$, two-way repeated measures ANOVA). This suggests a possible involvement of increased vasoconstriction in the initial stage of the exacerbation of Ang II–mediated hypertension in ATRAP-KO mice.

DISCUSSION

In this study it was demonstrated that systemic ATRAP deficiency does not exert any evident influence on baseline

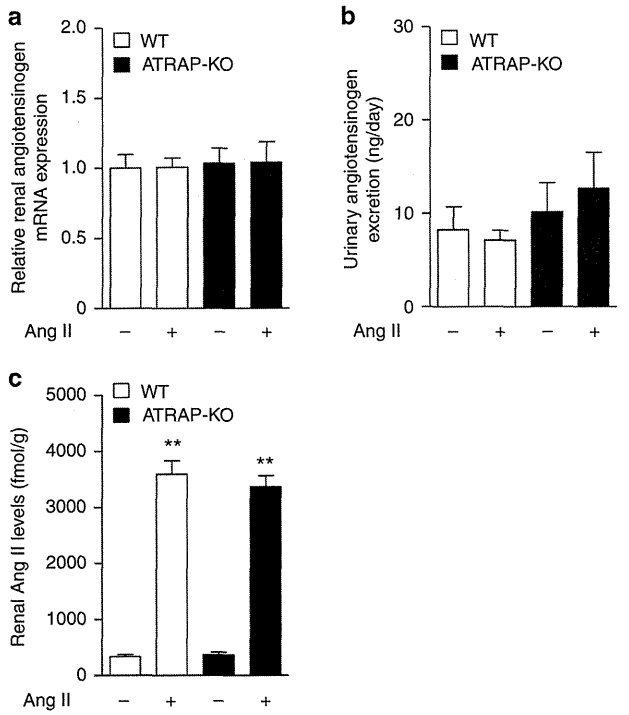

Figure 7 | Angiotensin II type 1 receptor (AT1R)-associated protein (ATRAP) deficiency exerts no apparent effects on renal angiotensinogen (AGT) production or renal angiotensin II (Ang II) levels. (**a**) Quantitative analysis of the mRNA expression of renal AGT in the wild-type (WT) and ATRAP-knockout (KO) mice. Values are expressed as mean ± s.e. ($n = 7$–9 in each group). (**b**) Urinary AGT excretion in WT and ATRAP-KO mice after administration of vehicle or Ang II (2000 ng/kg/min) for 14 days. Values are expressed as mean ± s.e. ($n = 6$–7 in each group). (**c**) Renal Ang II levels in WT and ATRAP-KO mice after administration of vehicle or Ang II for 14 days. Values are expressed as mean ± s.e. ($n = 7$–9 in each group).

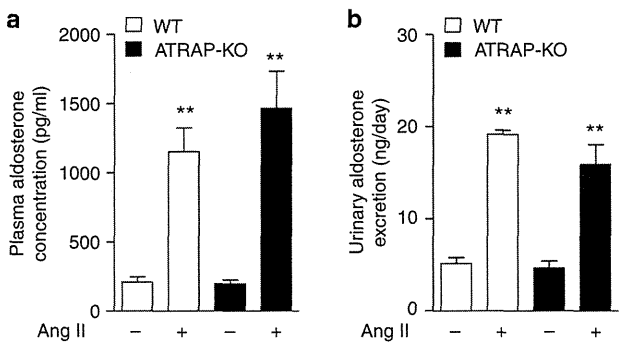

Figure 8 | Angiotensin II type 1 receptor (AT1R)-associated protein (ATRAP) deficiency did not affect plasma aldosterone concentration or urinary aldosterone excretion. (**a**) Plasma aldosterone concentration in wild-type (WT) and ATRAP-knockout (KO) mice after the administration of vehicle or Ang II (2000 ng/kg/min) for 14 days. Values are expressed as mean ± s.e. ($n = 6$ in each group). $^{**}P < 0.01$ versus vehicle. (**b**) Urinary aldosterone excretion in the WT and ATRAP-KO mice after administration of vehicle or Ang II for 14 days. Values are expressed as mean ± s.e. ($n = 5$–6 in each group). $^{**}P < 0.01$ versus vehicle.

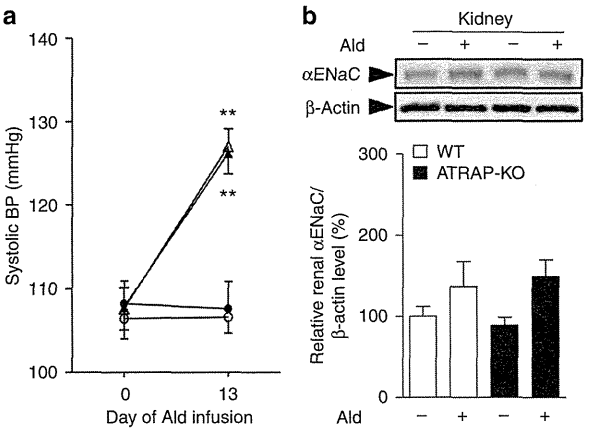

Figure 9 | Angiotensin II type 1 receptor (AT1R)-associated protein (ATRAP) deficiency exerts no significant influence on the aldosterone (Ald)-induced changes in blood pressure (BP) and renal α-subunit of the epithelial sodium channel (αENaC) expression. (**a**) Systolic BP was similarly increased by aldosterone (50 μg/kg/day) infusion for 14 days in wild-type (WT) and ATRAP-knockout (KO) mice that were fed a normal (0.3%) sodium diet, and maintained on 1% NaCl in the drinking water. Values are expressed as mean ± s.e. (n = 5 in each group). $^{**}P < 0.01$ versus vehicle. (**b**) Effects of aldosterone infusion on the protein expression of the αENaC in the kidneys of WT and ATRAP-KO mice. Values are expressed as mean ± s.e. ($n = 5$ in each group).

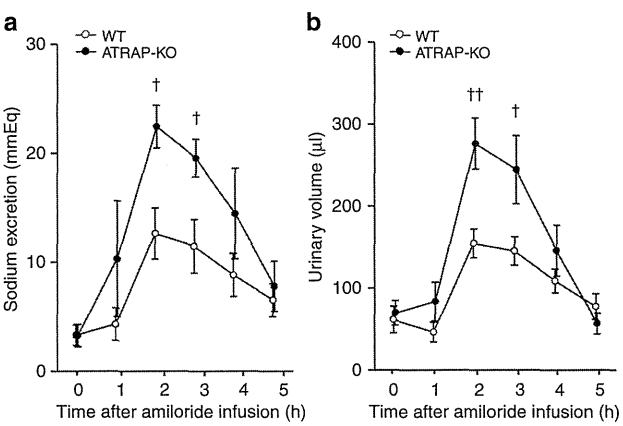

Figure 10 | Angiotensin II type 1 receptor (AT1R)-associated protein (ATRAP) deficiency causes reinforcement of the urinary sodium excretory effects of amiloride administered after chronic angiotensin II (Ang II) infusion. (**a**) Urinary sodium excretion after amiloride (3 mg/kg) infusion was significantly increased in the Ang II (2000 ng/kg/min)-infused ATRAP-knockout (KO) mice compared with the Ang II-infused wild-type (WT) mice. (**b**) Urine volume after amiloride (3 mg/kg) infusion was further elevated in the Ang II-infused ATRAP-KO mice compared with the Ang II-infused WT mice. Values are expressed as mean ± s.e. ($n = 5$–7 in each group). $^{\dagger}P < 0.05$ versus WT mice, $^{\dagger\dagger}P < 0.01$ versus WT mice.

BP upon radiotelemetry or on renal structure and function. This is in sharp contrast to the reported phenotypic changes in the genetic deletion of other RAS components (that is, AGT, renin, and AT1R). These RAS-inactivated mice

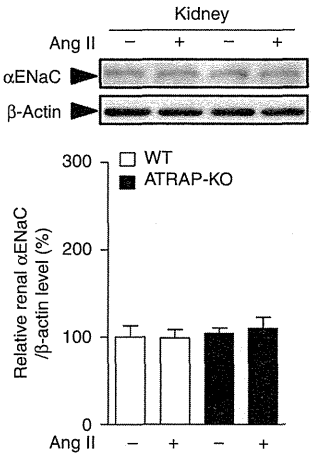

Figure 11 | The renal α-subunit of the epithelial sodium channel (αENaC) protein expression levels just after the start of angiotensin II (Ang) II infusion did not differ significantly between the wild-type (WT) and angiotensin II type 1 receptor (AT1R)-associated protein (ATRAP)-knockout (KO) mice. Effects of Ang II (2000 ng/kg/min) infusion for 1 day on protein expression of the αENaC in the kidneys of WT and ATRAP-KO mice. Values are expressed as mean ± s.e. ($n = 7$–8 in each group).

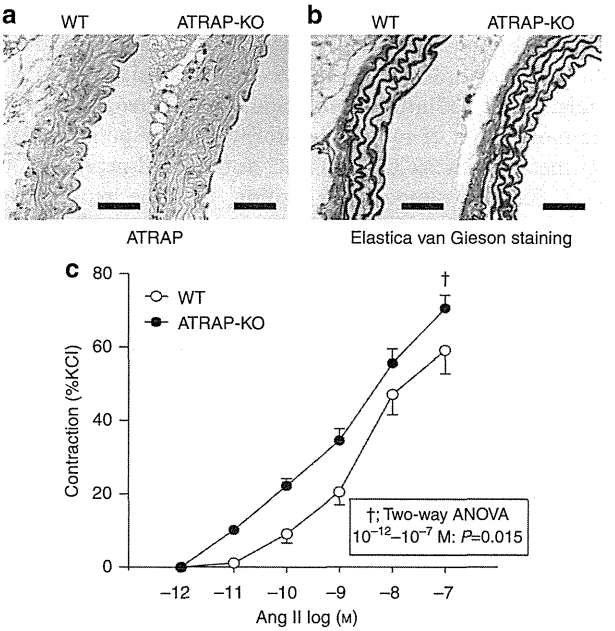

Figure 12 | Angiotensin II type 1 receptor (AT1R)-associated protein (ATRAP) deficiency enhances angiotensin II (Ang II)-induced vasoconstriction. (**a**) Immunohistochemistry for ATRAP in aorta sections from wild-type (WT) and ATRAP-knockout (KO) mice. The positive areas for ATRAP are evident as brown dots in the sections. Scale bar = 50 μm. Original magnification ×400. (**b**) Elastica van Gieson staining of representative aorta sections from WT and ATRAP KO mice. Scale bar = 50 μm. Original magnification ×400. (**c**) Ang II–induced vasoconstriction was significantly increased in the vascular ring of ATRAP-KO mice compared with that of WT mice. The concentration of Ang II was increased from 10^{-12} to 10^{-7} mol/l. Vasoconstriction responses to Ang II are expressed as the percentage of contraction induced by potassium-enriched solutions (22 mmol/l NaCl, 120 mmol/l KCl, 1.5 mmol/l CaCl2, 6 mmol/l glucose, 1 mmol/l $MgCl_2$, and 5 mmol/l HEPES, pH 7.4). Values are expressed as mean ± s.e. ($n = 6$ in each group). $^{\dagger}P < 0.05$ versus WT mice.

displayed significant decreases in baseline BP as well as pathological alterations in renal structure and function compared with the control mice.[11–15]

With respect to a possible effect of genetic alteration in ATRAP on BP regulation, a previous study examined phenotypic changes in systemic ATRAP gene-trap mice.[18] These mice have a gene-trap cassette with splicing acceptor in ATRAP intron 4 and exhibit fusion of ATRAP exons 1 to 4 with β-galactosidase/neomycin resistance gene, with an elevated baseline BP concomitant with an increased plasma volume and lowered urinary pH.[18] This previous study suggested an augmented baseline NHE3-dependent sodium reabsorption in proximal tubules of these mice, and the authors proposed a regulatory role for proximal tubule ATRAP in modulation of renal sodium handling and baseline BP.[18] However, the phenotypic difference in these ATRAP gene-trap mice might be because of aberrant ATRAP-gal/neo protein production. In addition, the strain of ATRAP gene-trap and control mice used for comparison were not reported,[18] thereby making it difficult to properly interpret their BP data. Furthermore, the previously reported systemic ATRAP transgenic mice (TGM) produced separately in both our laboratory and a distinct laboratory exhibited no baseline BP changes.[19,20] These findings support the results of the present study, showing an absence of BP change at baseline in ATRAP-KO mice.

In contrast to the lack of any evident change in baseline BP in ATRAP-KO mice, Ang II–mediated hypertension was significantly exacerbated in ATRAP-KO mice concomitant with an increased sodium balance compared with WT mice. With respect to the mechanisms involved in Ang II–induced hypertension, previous studies using a series of kidney cross-transplant experiments showed that activation of the intrarenal Ang II–AT1R axis is critically important for both Ang II–dependent hypertension and end-organ damage.[21–23]

Sodium reabsorption through renal proximal and distal tubules is reportedly regulated by the activity of the intrarenal Ang II–AT1R axis.[24] The proximal tubule AT1R directly affects BP regulation because a major portion of the glomerular filtrate is reabsorbed in proximal tubules, and proximal tubule sodium transport is considered a major determinant of the pressure natriuresis response.[25] The proximal tubule–specific AT1R-deficient mice exhibited a partial suppression of Ang II–induced BP elevation as well as a decrease in baseline BP compared with control mice, concomitant with Ang II–induced reduction in NHE3 expression.[26] On the other hand, another type of proximal tubule–specific AT1R-deficient mouse exhibited a significant reduction in baseline BP, but without any evident inhibition of Ang II–induced hypertension in comparison with control mice.[27] These results indicate that activation of AT1R signaling in renal proximal tubules is unable to fully account for the positive effect of Ang II on BP increase.

Regarding the role of distal tubules in renal sodium handling by the Ang II–AT1R axis, previous studies showed that distal nephron segments also have a crucial role in the regulation of sodium reabsorption via intrarenal RAS.[28,29] The modulation of sodium reabsorption in response to Ang II is mediated by NCC and ENaC in the distal nephron.[30–35] These findings support the notion that the renal distal tubules also have a role in sodium reabsorption that takes place in response to Ang II. Recently, we generated renal distal tubule–dominant ATRAP TGM (renal distal convoluted tubule-ATRAP TGM).[8] The renal distal convoluted tubule-ATRAP TGM exhibited a significant amelioration of Ang II–induced hypertension, in spite of no change in baseline BP, at least partly via a suppression of the upregulation of renal αENaC expression by Ang II stimulation,[8] thereby suggesting a regulatory role of distal tubule ATRAP in the regulation of renal sodium handling. With respect to the intrarenal distribution of ATRAP, its protein was found to be widely and abundantly expressed along both the proximal and distal tubules. Thus, it is important to determine which of the functional effects of renal tubule ATRAP (that is, proximal tubule ATRAP or distal tubule ATRAP) is more relevant to the regulation of renal sodium handling that modulates BP response under pathological conditions such as Ang II infusion.

In this study, the renal expression of NHE3, a major sodium transporter in proximal tubules, as well as of urinary pH, which reflects proximal tubule NHE3 activity, and renal AGT production (both mRNA expression and urinary excretion) were similar in WT and ATRAP-KO mice. These results suggest that sodium reabsorption by NHE3 in proximal tubules was not affected by ATRAP deficiency and an increase in sodium reabsorption in proximal tubules by Ang II–AT1R axis is not likely to play a major role in the exacerbation of Ang II–induced hypertension that occurs in ATRAP-KO mice. In addition, renal AGT production and renal Ang II content were similar with or without Ang II. The positive feedback loop of Ang II to its substrate AGT has been demonstrated in various tissues, including liver,[36,37] heart,[38,39] and adipose tissue.[40,41] However, in the kidney, the feedback loop of Ang II to AGT is regulated in a dose-dependent manner.[16,17,42,43] Although a low dose of Ang II infusion reportedly increases AGT levels in the kidney,[16] a high dose did not change them.[17] Accordingly, these results suggest that systemic ATRAP deficiency did not affect renal AGT production, resulting in an unaltered renal Ang II level.

On the other hand, the Ang II–induced stimulation of renal expression and activity of ENaC, a major sodium transporter in distal tubules, was significantly enhanced in ATRAP-KO mice compared with WT mice. Although aldosterone is one of the major positive regulators of ENaC, both the circulating and urinary aldosterone levels were comparable in the two groups, and the BP response and renal ENaC expression by chronic aldosterone infusion were not affected in ATRAP-KO mice, thereby excluding aldosterone as a major contributor to the enhancement of the Ang II–induced activation of ENaC.

ENaC is formed by three homologous subunits (α, β, and γ) and coexpression of all three subunits is needed to induce maximal channel activity, and αENaC has a critical role in the formation of a functional ion channel.[44,45] With respect to the possible direct effects of Ang II on ENaC, Ang II reportedly stimulates distal sodium transport activity via an upregulation of αENaC expression and an enhancement of ENaC activity by modulation of the probability of the channel being open.[35,46–49] A recent study has also shown that Ang II directly promotes translocation of αENaC to the apical plasma membrane and increases the number of functionally active channels *in vivo*.[50] Considering these reports, posttranslational modifications that alter trafficking or function of the channel, as well as an increase in αENaC expression, may contribute to the enhanced ENaC function that occurs in ATRAP-KO mice. Further studies are needed to investigate these possible mechanisms.

Finally, with respect to the mechanisms of the initiation process of exacerbation of Ang II–mediated hypertension in ATRAP-KO mice, although Ang II–induced sodium retention and BP elevation tended to be different between ATRAP-KO and WT mice even during the early phase of Ang II infusion, the renal αENaC protein expression level was comparable on day 1 of Ang II infusion. These findings suggest that changes in glomerular hemodynamics, glomerular filtration rate, and vasoconstriction may be involved in the differences in sodium balance and BP elevation that occur during the early phase of Ang II infusion. Indeed, Ang II induced greater vasoconstrictor responses in the vascular ring of ATRAP-KO mice than WT mice. Enhancement of Ang II–induced vasoconstriction because of ATRAP deficiency may be one of the mechanisms underlying the exacerbation of Ang II–mediated hypertension, particularly in the early initiation period.

In summary, these results indicate that the pathological activation of renal tubular AT1R in response to chronic Ang II infusion, which is enhanced by ATRAP deficiency, directly provokes ENaC activation in distal tubules, so as to promote sodium retention in an aldosterone-independent manner and to contribute to the exacerbation of Ang II–mediated hypertension. As we employed systemic ATRAP-KO mice in this study, it is not practical to examine the nephron segment–specific effect of ATRAP. Further investigation is needed to elucidate the *in vivo* functional roles of ATRAP in a nephron segment–specific manner, including its possible interaction with sodium transporters other than ENaC. Such investigation, including the use of conditional gene KO mice, will be taken up in due course.

MATERIALS AND METHODS

Targeted disruption of the gene encoding ATRAP/*Agtrap* in C57BL/6 mice

We employed a targeted gene disruption strategy to produce ATRAP-KO mice (C57BL/6) as described previously.[51] All experiments were performed with ATRAP-KO mice and their WT littermates. This study was performed in accordance with the National Institutes of

Health guidelines for the use of experimental animals. All animal studies were reviewed and approved by the Animal Studies Committee of Yokohama City University.

Quantitative real-time reverse transcriptase–PCR analysis

Quantitative real-time reverse transcriptase–PCR was performed using designed TaqMan probes (Agtrap, Mm00507771_m1; AT1R, Mm01957722_s1; NHE3, Mm01352473_m1; NKCC2, Mm01275821_m1; NCC, Mm00490213_m1; αENaC, Mm00803386_m1; βENaC, Mm00441215_m1; γENaC, Mm00441228_m1; and AGT, Mm00599662_m1; Applied Biosystems, Carlsbad, CA), as described previously.[8] The mRNA levels were normalized to those of the 18S rRNA control.

Histological and immunohistochemical analysis

Immunohistochemistry was performed as described previously.[10,20,52,53] The sections were incubated with one of the following: (1) anti-ATRAP antibody diluted to 1:100, (2) anti-aquaporin 2 antibody (1:200; 254-271, CALBIOCHEM, Darmstadt, Germany), (3) anti-calbindin D-28K antibody (1:3000; C9848, Sigma-Aldrich, St Louis, MO), or (4) anti-megalin antibody (1:1000; NB110-96417, Novus Biologicals, Littleton, CO).

Ang II infusion and BP measurement by radiotelemetric method

Direct BP measurement was performed by radiotelemetric method using a BP transducer (Model TA11PA-C10; Data Science International, New Brighton, MN) as described previously.[6,8,54] Ang II (500 or 2000 ng/kg/min) was infused subcutaneously into the mice via an osmotic minipump (Model 2002, ALZET, Palo Alto, CA) and hemodynamic measurements were recorded every 5 min using the software Dataquest A.R.T. 4.1 (Data Science International). Baseline BP values were the average of three consecutive days.

Metabolic cage analysis

All mice (male, 11 weeks of age) were fed a normal diet (0.3% NaCl) throughout this. Mice were acclimated for a week to metabolic cages (Techniplast, Buguggiate, Italy) before Ang II (2000 ng/kg/min) infusion. Body weight, food intake, and water intake were measured daily, and urine was collected.

Diuretic test

The diuretic test using a 0.3 mg/ml amiloride solution in 10% dimethyl sulfoxide was performed essentially as described previously.[55] After Ang II infusion (2000 ng/kg/min) for 14 days, mice were subsequently injected intraperitoneally with 40 μl/g saline to facilitate spontaneous voiding. At 1 h after saline injection, amiloride (3 mg/kg) was intraperitoneally injected. The dose of amiloride was determined based on a previous study.[56] Urine was collected every hour by spontaneous voiding or bladder massage, and urine volume and sodium excretion were measured.

Aldosterone infusion and BP measurement by tail-cuff method

Mice (male, 11 weeks of age), fed a normal diet (0.3% NaCl) with 1% NaCl in the drinking water, were subcutaneously infused with aldosterone (50 μg/kg/day) via an osmotic minipump for 14 days.[57,58] Measurement of systolic BP by the tail-cuff method (BP monitor MK-2000; Muromachi Kikai, Tokyo, Japan) was performed.[20,59]

Membranous protein extraction and immunoblot analysis for epithelial sodium transporters

Membranous proteins were extracted from kidneys using the Plasma Membrane Extraction Kit (K268-50; Biovision, Milpitas, CA), and immunoblot analysis was performed as described previously.[6,8,10,20] Antibodies against NHE3 (NHE31-A, Alpha Diagnostic International, San Antonio, TX), phospho-NKCC2 on Thr96 (kindly provided by Dr Shih-Hua Lin, Tri-Service General Hospital, Taipei, Taiwan),[60] phospho-NCC on Ser71,[61] αENaC (PA1-920A, Affinity Bioreagents, Golden, CO), βENaC (ENACb21-A, Alpha Diagnostic), and γENaC (ab3468, Abcam, Cambridge, UK) were used.

Biochemical assay

Plasma and urinary aldosterone concentrations were determined using the radioimmunoassay (RIA) kit (SPAC-S Aldosterone Kit; TFB, Tokyo, Japan). Urinary AGT level was determined using the sandwich enzyme-linked immunosorbent assay, as described previously.[62] Urinary creatinine, sodium, albumin, and serum creatinine were assessed using an autoanalyzer (Hitachi 7180; Hitachi, Tokyo, Japan). Urinary pH was determined with a pH glass electrode (TwinPH B-212; Horiba, Kyoto, Japan). Renal Ang II level was measured by RIA as described previously.[63]

Vessel wire myograph study

Isometric tension of aortic vascular rings from ATRAP-KO and WT mice was measured using a two-channel myograph (Dual Wire myograph system 410A; Unique Medical, Tokyo, Japan), as described previously.[64,65] The vascular rings were treated with Ang II (10^{-12} to 10^{-7} mol/l) and potassium-enriched solutions to stimulate vasoconstriction.

Statistical analysis

All data are shown as mean ± s.e. Differences were analyzed by Student's unpaired *t*-test or ANOVA for multiple comparisons. Differences between groups for categorical variables were analyzed using the χ^2-test. The *P*-values of <0.05 were considered statistically significant.

DISCLOSURE

All the authors declared no competing interests.

ACKNOWLEDGMENTS

This work was supported by a Health and Labor Sciences Research grant and by grants from the Japanese Ministry of Education, Science, Sports and Culture, the Salt Science Research Foundation (no. 1134), the Yokohama Foundation for Advancement of Medical Science, the Kidney Foundation, Japan (JKFB13-17), and the Novartis Foundation for Gerontological Research (2012).

REFERENCES

1. Guyton AC. Blood pressure control–special role of the kidneys and body fluids. *Science* 1991; **252**: 1813–1816.
2. Daviet L, Lehtonen JY, Tamura K *et al.* Cloning and characterization of ATRAP, a novel protein that interacts with the angiotensin II type 1 receptor. *J Biol Chem* 1999; **274**: 17058–17062.
3. Lopez-Ilasaca M, Liu X, Tamura K *et al.* The angiotensin II type I receptor-associated protein, ATRAP, is a transmembrane protein and a modulator of angiotensin II signaling. *Mol Biol Cell* 2003; **14**: 5038–5050.
4. Tanaka Y, Tamura K, Koide Y *et al.* The novel angiotensin II type 1 receptor (AT1R)-associated protein ATRAP downregulates AT1R and ameliorates cardiomyocyte hypertrophy. *FEBS Lett* 2005; **579**: 1579–1586.

5. Azuma K, Tamura K, Shigenaga A *et al.* Novel regulatory effect of angiotensin II type 1 receptor-interacting molecule on vascular smooth muscle cells. *Hypertension* 2007; **50**: 926–932.
6. Wakui H, Tamura K, Tanaka Y *et al.* Cardiac-specific activation of angiotensin II type 1 receptor-associated protein completely suppresses cardiac hypertrophy in chronic angiotensin II-infused mice. *Hypertension* 2010; **55**: 1157–1164.
7. Tamura K, Wakui H, Maeda A *et al.* The physiology and pathophysiology of a novel angiotensin receptor-binding protein ATRAP/Agtrap. *Curr Pharm Des* 2013; **19**: 3043–3048.
8. Wakui H, Tamura K, Masuda S *et al.* Enhanced angiotensin receptor-associated protein in renal tubule suppresses angiotensin-dependent hypertension. *Hypertension* 2013; **61**: 1203–1210.
9. Masuda S, Tamura K, Wakui H *et al.* Expression of angiotensin II type 1 receptor-interacting molecule in normal human kidney and IgA nephropathy. *Am J Physiol Renal Physiol* 2010; **299**: F720–F731.
10. Tsurumi Y, Tamura K, Tanaka Y *et al.* Interacting molecule of AT1 receptor, ATRAP, is colocalized with AT1 receptor in the mouse renal tubules. *Kidney Int* 2006; **69**: 488–494.
11. Tanimoto K, Sugiyama F, Goto Y *et al.* Angiotensinogen-deficient mice with hypotension. *J Biol Chem* 1994; **269**: 31334–31337.
12. Niimura F, Labosky PA, Kakuchi J *et al.* Gene targeting in mice reveals a requirement for angiotensin in the development and maintenance of kidney morphology and growth factor regulation. *J Clin Invest* 1995; **96**: 2947–2954.
13. Kihara M, Umemura S, Sumida Y *et al.* Genetic deficiency of angiotensinogen produces an impaired urine concentrating ability in mice. *Kidney Int* 1998; **53**: 548–555.
14. Oliverio MI, Kim HS, Ito M *et al.* Reduced growth, abnormal kidney structure, and type 2 (AT2) angiotensin receptor-mediated blood pressure regulation in mice lacking both AT1A and AT1B receptors for angiotensin II. *Proc Natl Acad Sci USA* 1998; **95**: 15496–15501.
15. Yanai K, Saito T, Kakinuma Y *et al.* Renin-dependent cardiovascular functions and renin-independent blood-brain barrier functions revealed by renin-deficient mice. *J Biol Chem* 2000; **275**: 5–8.
16. Kobori H, Harrison-Bernard LM, Navar LG. Expression of angiotensinogen mRNA and protein in angiotensin II-dependent hypertension. *J Am Soc Nephrol* 2001; **12**: 431–439.
17. Gonzalez-Villalobos RA, Seth DM, Satou R *et al.* Intrarenal angiotensin II and angiotensinogen augmentation in chronic angiotensin II-infused mice. *Am J Physiol Renal Physiol* 2008; **295**: F772–F779.
18. Oppermann M, Gess B, Schweda F *et al.* Atrap deficiency increases arterial blood pressure and plasma volume. *J Am Soc Nephrol* 2010; **21**: 468–477.
19. Oshita A, Iwai M, Chen R *et al.* Attenuation of inflammatory vascular remodeling by angiotensin II type 1 receptor-associated protein. *Hypertension* 2006; **48**: 671–676.
20. Wakui H, Tamura K, Matsuda M *et al.* Intrarenal suppression of angiotensin II type 1 receptor binding molecule in angiotensin II-infused mice. *Am J Physiol Renal Physiol* 2010; **299**: F991–F1003.
21. Coffman TM, Crowley SD. Kidney in hypertension: guyton redux. *Hypertension* 2008; **51**: 811–816.
22. Crowley SD, Gurley SB, Herrera MJ *et al.* Angiotensin II causes hypertension and cardiac hypertrophy through its receptors in the kidney. *Proc Natl Acad Sci USA* 2006; **103**: 17985–17990.
23. Crowley SD, Zhang J, Herrera M *et al.* Role of AT receptor-mediated salt retention in angiotensin II-dependent hypertension. *Am J Physiol Renal Physiol* 2011; **301**: F1124–F1130.
24. Kobori H, Nangaku M, Navar LG *et al.* The intrarenal renin-angiotensin system: from physiology to the pathobiology of hypertension and kidney disease. *Pharmacol Rev* 2007; **59**: 251–287.
25. McDonough AA, Leong PK, Yang LE. Mechanisms of pressure natriuresis: how blood pressure regulates renal sodium transport. *Ann NY Acad Sci* 2003; **986**: 669–677.
26. Gurley SB, Riquier-Brison AD, Schnermann J *et al.* AT1A angiotensin receptors in the renal proximal tubule regulate blood pressure. *Cell Metab* 2011; **13**: 469–475.
27. Li H, Weatherford ET, Davis DR *et al.* Renal proximal tubule angiotensin AT1A receptors regulate blood pressure. *Am J Physiol Regul Integr Comp Physiol* 2011; **301**: R1067–R1077.
28. Navar LG, Kobori H, Prieto MC *et al.* Intratubular renin-angiotensin system in hypertension. *Hypertension* 2011; **57**: 355–362.
29. Prieto-Carrasquero MC, Botros FT, Kobori H *et al.* Collecting duct renin: a major player in angiotensin II-dependent hypertension. *J Am Soc Hypertens* 2009; **3**: 96–104.
30. Castaneda-Bueno M, Cervantes-Perez LG, Vazquez N *et al.* Activation of the renal Na+:Cl- cotransporter by angiotensin II is a WNK4-dependent process. *Proc Natl Acad Sci USA* 2012; **109**: 7929–7934.
31. Christensen BM, Perrier R, Wang Q *et al.* Sodium and potassium balance depends on alphaENaC expression in connecting tubule. *J Am Soc Nephrol* 2010; **21**: 1942–1951.
32. Peti-Peterdi J, Warnock DG, Bell PD. Angiotensin II directly stimulates ENaC activity in the cortical collecting duct via AT(1) receptors. *J Am Soc Nephrol* 2002; **13**: 1131–1135.
33. San-Cristobal P, Pacheco-Alvarez D, Richardson C *et al.* Angiotensin II signaling increases activity of the renal Na-Cl cotransporter through a WNK4-SPAK-dependent pathway. *Proc Natl Acad Sci USA* 2009; **106**: 4384–4389.
34. van der Lubbe N, Lim CH, Fenton RA *et al.* Angiotensin II induces phosphorylation of the thiazide-sensitive sodium chloride cotransporter independent of aldosterone. *Kidney Int* 2011; **79**: 66–76.
35. Zhao D, Seth DM, Navar LG. Enhanced distal nephron sodium reabsorption in chronic angiotensin II-infused mice. *Hypertension* 2009; **54**: 120–126.
36. Klett C, Bader M, Ganten D *et al.* Mechanism by which angiotensin II stabilizes messenger RNA for angiotensinogen. *Hypertension* 1994; **23**: I120–I125.
37. Brasier AR, Li J. Mechanisms for inducible control of angiotensinogen gene transcription. *Hypertension* 1996; **27**: 465–475.
38. Herrmann HC, Dzau VJ. The feedback regulation of angiotensinogen production by components of the renin-angiotensin system. *Circ Res* 1983; **52**: 328–334.
39. Tamura K, Umemura S, Nyui N *et al.* Activation of angiotensinogen gene in cardiac myocytes by angiotensin II and mechanical stretch. *Am J Physiol* 1998; **275**: R1–R9.
40. Hainault I, Nebout G, Turban S *et al.* Adipose tissue-specific increase in angiotensinogen expression and secretion in the obese (fa/fa) Zucker rat. *Am J Physiol Endocrinol Metab* 2002; **282**: E59–E66.
41. Lu H, Boustany-Kari CM, Daugherty A *et al.* Angiotensin II increases adipose angiotensinogen expression. *Am J Physiol Endocrinol Metab* 2007; **292**: E1280–E1287.
42. Schunkert H, Ingelfinger JR, Jacob H *et al.* Reciprocal feedback regulation of kidney angiotensinogen and renin mRNA expressions by angiotensin II. *Am J Physiol* 1992; **263**: E863–E869.
43. Ingelfinger JR, Jung F, Diamant D *et al.* Rat proximal tubule cell line transformed with origin-defective SV40 DNA: autocrine ANG II feedback. *Am J Physiol* 1999; **276**: F218–F227.
44. Canessa CM, Schild L, Buell G *et al.* Amiloride-sensitive epithelial Na+ channel is made of three homologous subunits. *Nature* 1994; **367**: 463–467.
45. Pratt JH. Central role for ENaC in development of hypertension. *J Am Soc Nephrol* 2005; **16**: 3154–3159.
46. Beutler KT, Masilamani S, Turban S *et al.* Long-term regulation of ENaC expression in kidney by angiotensin II. *Hypertension* 2003; **41**: 1143–1150.
47. Mamenko M, Zaika O, Ilatovskaya DV *et al.* Angiotensin II increases activity of the epithelial Na+ channel (ENaC) in distal nephron additively to aldosterone. *J Biol Chem* 2012; **287**: 660–671.
48. Sun P, Yue P, Wang WH. Angiotensin II stimulates epithelial sodium channels in the cortical collecting duct of the rat kidney. *Am J Physiol Renal Physiol* 2012; **302**: F679–F687.
49. Zaika O, Mamenko M, Staruschenko A *et al.* Direct activation of ENaC by Angiotensin II: recent advances and new insights. *Curr Hypertens Rep* 2013; **15**: 17–24.
50. Mamenko M, Zaika O, Prieto MC *et al.* Chronic angiotensin II infusion drives extensive aldosterone-independent epithelial Na+ channel activation. *Hypertension* 2013; **62**: 1111–1122.
51. Maeda A, Tamura K, Wakui H *et al.* Angiotensin receptor-binding protein ATRAP/Agtrap inhibits metabolic dysfunction with visceral obesity. *J Am Heart Assoc* 2013; **2**: e000312.
52. Sato K, Kihara M, Hashimoto T *et al.* Alterations in renal endothelial nitric oxide synthase expression by salt diet in angiotensin type-1a receptor gene knockout mice. *J Am Soc Nephrol* 2004; **15**: 1756–1763.
53. Matsuda M, Tamura K, Wakui H *et al.* Involvement of Runx3 in the basal transcriptional activation of the mouse angiotensin II type 1 receptor-associated protein gene. *Physiol Genomics* 2011; **43**: 884–894.
54. Wakui H, Dejima T, Tamura K *et al.* Activation of angiotensin II type 1 receptor-associated protein exerts an inhibitory effect on vascular hypertrophy and oxidative stress in angiotensin II-mediated hypertension. *Cardiovasc Res* 2013; **100**: 511–519.